Evaluation of European air quality modelled by CAMx including the volatility basis set scheme

G. Ciarelli[1], S. Aksoyoglu[1], M. Crippa[1,*], J. L. Jimenez[2,3], E. Nemitz[4], K. Sellegri[5], M. Äijälä[6], S. Carbone[7,], C.Mohr[8], C. O'Dowd[9], L. Poulain[10], U. Baltensperger[1], and A. S. H. Prévôt[1]**

[1]{Paul Scherrer Institute, Laboratory of Atmospheric Chemistry, 5232 Villigen PSI, Switzerland}

[2]{Cooperative Institute for Research in Environmental Sciences, University of Colorado, Boulder, CO 80309, USA}

[3]{Department of Chemistry and Biochemistry, University of Colorado, Boulder, CO 80309, USA}

[4]{Center for Ecology and Hydrology, Bush Estate, Penicuik, Midlothian, EH26 0QB, UK}

[5]{Laboratoire de Météorologie Physique CNRS UMR6016, Observatoire de Physique du Globe de Clermont-Ferrand, Université Blaise Pascal, 63171 Aubière, France}

[6]{University of Helsinki, Department of Physics, Helsinki, Finland}

[7]{Atmospheric Composition Research, Finnish Meteorological Institute, P.O. Box 503, 00101 Helsinki, Finland}

[8]{Karlsruhe Institute of Technology, Institute of Meteorology and Climate Research, Germany}

[9]{School of Physics and Centre for Climate & Air Pollution Studies, Ryan Institute, National University of Ireland Galway, University Road, Galway, Ireland}

[10]{Leibniz-Institute for Tropospheric Research (TROPOS), Permoserstr. 15, 04318 Leipzig, Germany}

[*]{now at: Joint Research Centre, Institute for Environment and Sustainability, I-21020 Ispra (Va) JRC, Italy}

[**]{now at: Institute of Physics, University of São Paulo, Rua do Matão Travessa R, 187, 05508-090 São Paulo, S.P., Brazil}

Correspondence to: S. Aksoyoglu (sebnem.aksoyoglu@psi.ch)

Abstract

Four periods of EMEP (European Monitoring and Evaluation Programme) intensive measurement campaigns (June 2006, January 2007, September-October 2008 and February-March 2009) were modelled using the regional air quality model CAMx with VBS (Volatility Basis Set) approach for the first time in Europe within the framework of the EURODELTA-III model intercomparison exercise. More detailed analysis and sensitivity tests were performed for the period of February-March 2009 and June 2006 to investigate the uncertainties in emissions as well as to improve the modelling of organic aerosols (OA). Model performance for selected gas phase species and $PM_{2.5}$ was evaluated using the European air quality database Airbase. Sulfur dioxide (SO_2) and ozone (O_3) were found to be overestimated for all the four periods with O_3 having the largest mean bias during June 2006 and January-February 2007 periods (8.9 pbb and 12.3 ppb mean biases, respectively). In contrast, nitrogen dioxide (NO_2) and carbon monoxide (CO) were found to be underestimated for all the four periods. CAMx reproduced both total concentrations and monthly variations of $PM_{2.5}$ for all the four periods with average biases ranging from -2.1 $\mu g\ m^{-3}$ to 1.0 $\mu g\ m^{-3}$. Comparisons with AMS (aerosol mass spectrometer) measurements at different sites in Europe during February-March 2009 showed that in general the model over-predicts the inorganic aerosol fraction and under-predicts the organic one, such that the good agreement for $PM_{2.5}$ is partly due to compensation of errors. The effect of the choice of volatility basis set scheme (VBS) on OA was investigated as well. Two sensitivity tests with volatility distributions based on previous chamber and ambient measurements data were performed. For February-March 2009 the chamber-case reduced the total OA concentrations by about 42% on average. On the other hand, a test based on ambient measurement data increased OA concentrations by about 42% for the same period bringing model and observations into better agreement. Comparison with the AMS data at the rural Swiss site Payerne in June 2006 shows no significant improvement in modelled OA concentration. Further sensitivity tests with increased biogenic and anthropogenic emissions suggest that OA in Payerne were affected by changes in emissions from residential heating during the February-March 2009 whereas it was more sensitive to biogenic precursors in June 2006.

1 Introduction

Air pollution is known to cause damage to human health, vegetation and ecosystems. It is one of the main environmental causes of premature death. Only in Europe, more than 400,000 premature deaths were estimated in 2011 with $PM_{2.5}$ (particles less than 2.5 μm in aerodynamic diameter) having the highest relative risk for health damage (WHO, 2014a). Air quality models help understanding the processes taking place between emission sources and pollutant concentrations at receptor sites. They are very useful to define control strategies for future legislation. In spite of large improvements in recent years, Chemical Transport Models (CTMs) have still some uncertainties (Solazzo et al., 2012a). Various air quality model intercomparison exercises were successfully carried out over the last decades to determine uncertainties in chemical and physical processes governing particulate matter and its precursors (Solazzo et al., 2012a; Bessagnet et al., 2014). However, a large variability in particulate matter concentrations was found between different models indicating process parameterization as one of the main reasons for such discrepancies. Moreover, recent studies based on AMS (Aerosol Mass Spectrometer) measurements at different sites in Europe, revealed that the organic fraction dominates the non-refractory PM_1 composition (Crippa et al., 2014). Organic aerosol (OA) can be found in the atmosphere from direct emission by various sources, such as fossil fuel combustion by road vehicle engines or residential wood combustion. Direct emissions of OA are typically referred to as primary organic aerosol (POA) whereas gas-to-particle conversion is referred to as secondary organic aerosol (SOA). Formation mechanisms of SOAs are not very well known yet and their representation in CTMs is still challenging (Hallquist et al. 2009; Fountoukis et al., 2011; Bergstrom et al., 2012; Li et al., 2013; Langmann et al., 2014; Tsigaridis et al., 2014). In one of our recent aerosol modelling studies we compared model $PM_{2.5}$ prediction with PM_1 AMS measurements for different sites (Payerne and Zürich) and periods (summer and winter) in Switzerland. We found that particulate matter was generally well reproduced by the model with the SOA fraction being under-predicted and POA over-predicted (Aksoyoglu et al., 2011). Traditional CTMs treat POA as non-volatile. Some studies however have revealed the semi-volatile nature of POA, through its dynamic equilibrium of organic aerosol with its gas phase, and the importance of semi-volatile (SVOC) and intermediate volatility (IVOC) organic compounds as SOA precursors (Donahue et al., 2006; Robinson et al., 2007; Cappa and Jimenez, 2010). To describe the absorptive partitioning and ongoing oxidation of the atmospheric material, a volatility basis set (VBS) where organic species are organized into

surrogates according to their volatility was developed (Donahue et al., 2011, 2012a,b). Air quality models updated with VBS scheme started being used (Lane et al., 2008; Murphy and Pandis, 2009; Hodzic et al., 2010; Fountoukis et al., 2011; Bergström et al., 2012; Murphy et al., 2012; Jo et al., 2013; Zhang et al., 2013; Athanasopoulou et al., 2013; Fountoukis et al., 2014). Bergström et al. (2012) reported an EMEP model study over Europe for the 2002-2007 period using different assumptions regarding partitioning and aging processes. They could not reproduce the measured OA levels in winter suggesting that residential wood combustion inventories might be underestimated in different parts of Europe. Fountoukis et al. (2014) applied the PMCAMx model to simulate EUCAARI (Kulmala et al., 2009, 2011) and EMEP (Tørseth et al., 2012) campaigns in Europe. They could reproduce most of PM_1 daily average OA observations within a factor of two, with the February-March 2009 period having the largest discrepancies. Zhang et al. (2013) deployed the CHIMERE model with the VBS framework during the MEGAPOLI summer campaign in the Greater Paris region for July 2009. They found a considerable improvement in predicted SOA concentrations which might be even overestimated depending on the emission inventory used. In our study, we applied the regional air quality model CAMx with the VBS scheme for the first time in Europe within the framework of EURODELTA-III model intercomparison exercise. In addition to the base case configuration used in the exercise, more sensitivity tests with the VBS scheme for winter and summer episodes were performed together with a general evaluation of the four EMEP field measurement campaigns.

2 Method

2.1 The EURODELTA-III exercise

The EURODELTA-III (EDIII) framework is a European model intercomparison exercise between several modelling teams sharing both efforts and technical knowledge in order to reduce model uncertainties and to improve understanding of the performances. It contributes to the scientific work of the United Nations Economic Commission for Europe (UNECE) Task Force on Measurement and Modelling (TFMM) within the Convention on Long-range Transboundary Air Pollution (CLRTAP). In the first phase of the EDIII exercise, 4 periods of the EMEP field measurement campaigns were chosen in order to evaluate the model results:

- 1 June – 30 June 2006
- 8 January – 4 February 2007
- 17 September – 15 October 2008

- 25 February – 26 March 2009

Multiple models were applied on a common domain and driven with the same input data provided by the National Institute for Industrial Environment and Risks (INERIS). However, for some models, different meteorology, boundary conditions and emissions data such as biogenic emissions were used (Bessagnet et al., 2014).

2.2 Modelling method

2.2.1 CAMx

The Comprehensive Air quality Model with extensions, CAMx-VBS (CAMx5.41_VBS, kindly provided by ENVIRON before its public release) was used in this study. The model domain consisted of one grid with a horizontal resolution of 0.25° x 0.25°. The latitude and longitude grid extended from 25.125°W to 45.125°E and 29.875°N to 70.125°N resulting in 281 x 161 grid cells covering the whole of Europe. Hourly four-dimensional meteorological fields for wind speed and direction, pressure, temperature, specific humidity, cloud cover and rain required by CAMx simulations were calculated from ECMWF IFS (Integrated Forecast System) data at 0.2° resolution. Vertical diffusivity coefficients were estimated following the Kz approach of O'Brien (1970) using PBL depth profiles as available in IFS data. CAMx simulations used 33 terrain-following σ-levels up to about 8000 m above ground level, as in the original IFS data. The lowest layer was about 20 m thick. MACC (Monitoring Atmospheric Composition and Climate) reanalysis data were used to initialize initial and the boundary condition fields (Benedetti et al., 2009; Inness et al., 2013). Elemental carbon, organic aerosol, dust and sulfate were used to model aerosol species at the boundaries of the domain. One half of the OA was assumed to be secondary organic aerosol (SOA) and the other half primary organic aerosol (POA), as recommended in the EDIII exercise. Photolysis rate inputs were calculated using the TUV radiative transfer and photolysis model (Madronich, 2002). The required ozone column densities to determine the spatial and temporal variation of the photolysis rates were extracted from TOMS data (NASA/GSFC, 2005). Removal processes as dry and wet deposition were simulated using the Zhang resistance model (Zhang et al., 2003) and a scavenging model approach for both gases and aerosols (ENVIRON, 2011), respectively. For the gas phase chemistry the Carbon Bond (CB05) mechanism (Yarwood et al., 2005) with 156 reactions and up to 89 species was used.

Partitioning of inorganic aerosols (sulfate, nitrate, ammonium, sodium and chloride) was performed using the ISORROPIA thermodynamic model (Nenes et al., 1998). Aqueous sulfate and nitrate formation in cloud water was simulated as well using the RADM aqueous chemistry algorithm (Chang et al., 1987).

2.2.2 Emissions

Anthropogenic emissions

Annual total gridded anthropogenic emissions were prepared and provided by INERIS for the EDIII exercise, which is based on a merging process of data-bases from different sources, i.e. TNO-MACC (Kuenen et al., 2011), EMEP (Vestreng et al., 2007), GAINS (The Greenhouse Gas and Air Pollution Interactions and Synergies). For specific countries where TNO-MACC emissions were missing (Iceland, Liechtenstein, Malta and Asian countries), the EMEP 0.5° × 0.5° emissions were used and re-gridded using adequate proxies such as "artificial land-use" and EPER (European Pollutant Emission Register) data (http://www.eea.europa.eu/) for industries. Total primary particle emissions were made available by EMEP in two different size ranges: below 2.5µm (fine) and between 2.5µm and 10µm (coarse). Total emissions were later split to estimate the amount of elemental carbon, and organic matter for each of the 10 SNAP codes (Selected Nomenclature for Air Pollution) and country. The final emission inventory thus compiled consisted of 6 gas species namely methane, carbon monoxide, ammonia, sulfur oxides, non-methane volatile organic compounds and nitrogen oxides and 6 categories of particulate matter classes: fine elemental carbon (EC2.5), coarse elemental carbon (EC10), fine primary organic material (fine POA), coarse primary organic material (coarse POA), fine other primary particulate material (non-carbonaceous) and coarse other primary particulate material (non-carbonaceous). $PM_{2.5}$ and PM_{10} emissions were provided by EMEP and they were split to elemental carbon and organic matter using the fractions given by IIASA (International Institute for Applied Systems Analysis) for each source and country. Total non-methane volatile organic compounds were split for the CB05 mechanism using the recommendations of Passant (2002). Hourly, weekly and monthly time profiles as in the EURODELTAII exercise were applied to total annual anthropogenic emissions.

Biogenic emissions

Biogenic VOC emissions were calculated using the Model of Emissions of Gases and Aerosols from Nature MEGANv2.1 (Guenther et al., 2012). This model is driven by meteorological variables such as hourly temperature, solar radiation, humidity, wind speed, soil moisture and land cover data including leaf area index (LAI) and plant function type (PFT) as available in the Community Land Model 4.0. 8-Days average satellite data at 0.25° x 0.25° resolution were pre-processed and made available from the TERRA/MODIS satellite system. Sixteen plant function types including needle-leaved evergreen, needle-leaved deciduous, broad-leaved evergreen, broad-leaved deciduous, grass and crop for different climatic zones were prepared for this study at 0.25° x 0.25° resolution together with the global emission factors of α-pinene, β-pinene, 3-carene, isoprene, limonene, 232-methylbutenol, myrcene, NO_x, *t-β*-ocimene and sabinene. Common BVOC species such as isoprene, terpene, sesquiterpene, xylene and toluene were obtained for each hour and cell in the domain.

2.2.3 VBS scheme

A new volatility basis set (VBS) scheme is available in the CAMx model to describe changes in oxidation state and volatility. A total of four basis set simulates the evolution of organic aerosol in the atmosphere (Koo et al., 2014). POA emissions were split in HOA-like and BBOA-like emissions and allocated in two different basis sets. HOA-like emissions include emissions from all SNAP sectors except SNAP2 (non-industrial combustion plants) and SNAP10 (agriculture) which were assigned to BBOA-like emissions. Two other sets were used in the model to allocate secondary organic aerosol from anthropogenic (i.e. xylene and toluene) (ASOA) and biogenic (i.e. isoprene, monoterpene and sesquiterpene) (BSOA) gaseous precursors. These two sets also allocate oxidation products of POA vapours, from each of the two primary sets (HOA-like and BBOA-like). The 2D volatility space retrieved by Donahue et al. (2011; 2012a,b) was used to distribute the organic molecular structures for each of the volatility bins and different sets (Table S1). Five volatility bins represent the range of semi-volatile organic compounds (SVOCs) ranging from 10^{-1} μg m^{-3} to 10^{3} μg m^{-3} in saturation concentrations (C*). Oxidation processes are modelled by shifting C* by a factor of 10 in the next lower volatility bin, increasing the oxidation state and reducing the carbon number to account for fragmentation. OH reaction rates are assumed to be 4 x 10^{-11} cm^3 $molecule^{-1}$ s^{-1} for the reaction of semi-volatile primary vapors with OH and 2 x 10^{-11} for further aging of ASOA and POA vapours from HOA-like emissions. More details about the

VBS parameterization in CAMx can be found in Koo et al. (2014). Further aging of BSOA is not considered in this study based on previous modelling results showing over-prediction of OA when such process is taken into account (Lane et al., 2008; Murphy and Pandis, 2009). This implies that also further aging of POA vapours from BBOA-like emissions was not considered since it is performed in the same basis set. In this work we focus on the effects of a VBS framework on the total OA fraction. Aging processes and alternative VBS implementations will be discussed together with SOA and POA components in a following paper (Ciarelli et al. in prep). Three sensitivity tests were performed with different assumptions on the volatility distributions (Table 1):

- **NOVBS:** Primary organic aerosol was assumed to be non-volatile. Biogenic (isoprene, monoterpenes and sesquiterpenes) and anthropogenic (xylene, toluene and other aromatics) volatile organic compounds (VOCs) were used as precursors for secondary organic aerosol. Partitioning of condensable gases to secondary organic aerosol was calculated using a semi-volatile equilibrium approach (Strader, 1999).

- **VBS_ROB:** Primary organic aerosol was assumed to be volatile and undergo chemical oxidation. The volatility distribution estimated by Robinson et al. (2007) was applied to HOA-like and BBOA-like emissions. Emissions of intermediate volatility organic compounds (IVOCs) were assumed to be 1.5 times those of primary organic aerosol (POA) as suggested by Robinson et al. (2007).

- **VBS_BC:** Primary organic aerosol was assumed to be volatile and undergo chemical oxidation using the approach of Shrivastava et al. (2011) and Tsimpidi et al. (2010). The total primary emissions are roughly 3 times higher than in **VBS_ROB.** Different volatility distributions were applied for HOA and BBOA-like emissions. IVOCs were assumed to be 1.5 times the amount of POA. This implies that for this scenario the SVOC + IVOC mass added is equal to 7.5 times the initial amount of POA. This represents the base case scenario used to evaluate gas phase and $PM_{2.5}$ model performance.

Based on the **VBS_BC** base case scenario, two other sensitivity tests were performed with respect to emissions:

- **VBS_BC_2xBVOC:** Increased BVOCs emissions by a factor of 2.

- **VBS_BC_2xBBOA:** Increased BBOA-like emissions by a factor of 2.

2.3 Statistical methods

Statistical procedures as available in the Atmospheric Model Evaluation Tool (AMET, Apple et al., 2010) were used in this study to evaluate model performance. Daily ambient measurements of main gas phase species i.e. O_3, NO_2, CO, SO_2 and fine particulate matter ($PM_{2.5}$) were extracted from the Airbase database in Europe and statistics reported in terms of mean bias (MB), mean error (ME), mean fractional bias (MFB) mean fractional error (MFE) and correlation coefficient (r).

Due to the coarse grid resolution, only rural-background stations, defined as stations far from city sources of air pollution with pollution levels determined by the integrated contribution from all sources upwind of the station (ETC/ACC, 2004/7), with at least 80% daily average observations available were considered for the statistical analysis. For $PM_{2.5}$ this resulted in 48 stations available for June 2006, 56 for January-February 2007, 90 for September-October 2008 and 110 stations for February-March 2009. $PM_{2.5}$ components were further evaluated for the February-March 2009 period where comprehensive high resolution AMS measurements at 11 European sites were available, i.e., at Barcelona, Cabauw, Chilbolton, Helsinki, Hyytiälä, Mace Head, Melpitz, Montseny, Payerne, Puy de Dôme and Vavihill (Crippa et al., 2014).

3 Results and discussions

3.1 Model evaluation

Model performance metrics for gas phase species CO, NO_2, O_3 and SO_2 as well as for $PM_{2.5}$ are reported in Table 2 and they refer to the base case VBS_BC.

NO_2 and O_3

NO_2 was found to be under-predicted for all the four periods with mean fractional bias between -54% and -28% and NO_2 concentrations being particularly under-predicted during June 2006. Evaluation of the EURODELTA III model inter-comparison exercise showed that all models performed similarly for NO_2 in terms of correlation with *r* values in the range 0.6-0.7 and the spatial correlation was much higher in the range 0.7-0.9 for all models (Bessagnet et al., 2016) with a general underestimation in the afternoon. The NO_2 performance could be influenced by several factors:

- Uncertainties in the emission inventories. Although NO_x emission estimates in Europe are thought to have an uncertainty of about ± 20%, the complete data set used in the inventories has much higher uncertainty (Kuenen et al., 2014). A recent study identified a significant discrepancy between emission estimates and actual flux measurements, with the highest underestimation being a factor of two in central London mainly due to under-representation of real world road traffic emissions (Vaughan et al., 2016)

- The relatively coarse resolution of the domain which may result in too low NO_x emissions or isolated local events that the model cannot resolve. We report daily average time series of NO_2 for the period of Feb-Mar 2009 for stations in Table 2 as well as daily average time series of NO_2 for stations not exceeding 5 ppb (which represents 92% of the stations in Table 2) (Figure S1). The model performance for NO_2 significantly improved when the 5 ppb threshold was applied to the dataset. An emission map of NO for 1 March 2009 at 6 AM is reported in Figure S2. High emissions of NO are predicted in the Benelux area, Po Valley, Germany and in some of the eastern European countries. High NO emissions due to ship traffic are also visible especially in the Mediterranean Sea

- Possible positive artefacts in the chemiluminescence methods for measuring NO_2 may also occur when NO_2 is catalytically converted to NO on the molybdenum surface leading to an over-prediction of measured NO_2 concentrations (Steinbacher et al., 2007; Villena et al., 2012)

- Moreover, an evaluation of planetary boundary layer height (PBLH) within the EDIII shows that although the PBLH was quite well represented in general in the ECMWF IFS meteorological fields, CAMx tends to under-estimate the night-time minima and to over-estimate some daytime peaks, over-predicting the dilution of day time NO_2 concentrations, whereas the wind speed was relatively well reproduced (Bessagnet et al., 2016).

O_3 concentrations were found to be over-predicted for all the four periods with a mean fractional bias ranging from 2% to 48%. Especially in June 2006, when the photochemical activity is higher, the general under-prediction of NO_x in the whole domain reduces the O_3 titration potential during night time.

Model performance for O_3 is also strongly influenced by long-range transport especially during the winter periods when the local chemical production of O_3 is limited. Figure S3 shows the model performance at the Mace Head station located on the west coast of Ireland for all the four periods. Especially in January-February 2007 O_3 concentrations were found to be over-predicted by about 10 to 20 ppb indicating that boundary conditions for O_3 were probably not well represented. In June 2006 and September-October 2008 O_3 was relatively well captured at Mace Head suggesting that the observed positive bias in O_3 concentrations might arise from insufficient NO_x emissions to undergo titration during night time as well as not correctly represented planetary boundary layer dynamics. In February-March 2009 the model tends to under-predict the O_3 concentration at Mace Head and overall the O_3 model performance shows the lowest bias (2%). Eventually, the under-prediction of O_3 in the boundary condition may counteract the already mentioned deficiencies related to insufficient NO_x emissions.

SO_2 and CO

SO_2 concentrations were found to be slightly over-predicted for all the four periods with a mean fractional bias ranging from 14% to 36% for SO_2. The daily variations of modelled and measured SO_2 concentrations for February-March 2009 are reported as well in Figure S1 (lower-panel) for the stations in Table 2. In general, the daily variations of modelled and measured SO_2 concentrations agree relatively well with each other throughout the period.

Most of the SO_2 emissions arise from high stack point sources which have injection heights of a few hundred meters. It might be that the vertical distribution of SO_2 might affect the model performance in particular near the harbors and coastal areas where ship emissions were allocated in the second layer of the model domain (extending from ~20 to 50 m above ground level) whereas they can reach up to 58 meters in deep draft vessels (SCG, 2004) and also undergo plume rise. Insufficient conversion to sulfate or too low deposition processes might also positively bias the model performance for SO_2.

CO was slightly under-predicted for all periods (mean fractional bias between -11% and -31%), with highest values during the September-October 2008 period (-31%). The late summer-fall period is known to be influenced by agricultural open field burning activities which might be missing from standard emission inventories.

In general, for both SO_2 and CO, the model showed lower correlation coefficients with respect to other gas-phase species (*r* values from 0.20 and 0.37 for CO and from 0.37 to 0.52 for SO_2).

$PM_{2.5}$

Of all investigated variables, CAMx shows the best statistical performance for $PM_{2.5}$. For all four periods the acceptable model performance criteria recommended by Boylan and Russell (2006) for aerosols were met (MFE ≤ +75 % and −60 % < MFB < +60 %). The fractional bias ranges from less than 1% in September-October 2008 up to -13% in February-March 2009. Also the recommended model performance goals (MFE ≤ +50% and -30% < MFB < +30%) were met for all periods except for January 2007. Modelled average $PM_{2.5}$ concentrations are shown in Fig. 1. A different spatial distribution is seen for summer and winter. In June 2006 the model predicts higher concentrations in the southern part of the domain especially over the Mediterranean Sea and North Africa (up to 35 μg m^{-3}). On the other hand, the highest concentrations were predicted in the Po valley area (above 40 μg m^{-3}) and in the southern part of Poland during January-February 2007. During the two colder periods (2007 and 2009) elevated concentrations of around 15 μg m^{-3} are also visible close to urban areas such as Paris and Moscow. Figure 2 shows $PM_{2.5}$ variations at Airbase rural-background sites in terms of medians, 25^{th} and 75^{th} percentiles. In all the four periods CAMx is able to reproduce the observed monthly variation very well with some over-prediction occurring mainly from the 14^{th} to the 17^{th} of January 2007 and towards the end of 2008 period.

3.2 Detailed evaluation of $PM_{2.5}$ components in February-March 2009

The modelled concentrations of non-refractory $PM_{2.5}$ components were compared against aerosol mass spectrometer measurements at eleven European sites for the February-March 2009 period (Crippa et al., 2014). Even though the AMS measures particles with a diameter *D* < 1 μm, the difference between the non-refractory PM_1 and total $PM_{2.5}$ mass is in general rather small as shown in Aksoyoglu et al. (2011), at least for situations without exceedingly high air pollution and situations when sea salt makes large relative contribution to $PM_{2.5}$. The modelled average total non-refractory $PM_{2.5}$ (sum of nitrate, sulfate, ammonium and OA) concentrations match the measurements quite well with a few exceptions (Fig. 3 and Table 3). The model is able to reproduce both high concentrations observed at the urban site Barcelona and low ones at remote sites like Hyytiälä, Finland. Concentrations of inorganic aerosols are

over-predicted and OA are under-predicted at most of the stations (with similar behavior during the other investigated periods, Figure S4 and Figure S5). Very similar results were also presented by other recent studies (Knote et al., 2011). The effect of different schemes to treat OA is discussed in Sect. 3.3. At the Cabauw site nitrate was the most dominant species (Mensah et al., 2012). Especially at this site the model strongly over-predicts in particular the nitrate (NO_3^-) fraction (by a factor of 3). A sensitivity test with 50% reduction in ammonia emissions significantly improved the modelled NO_3^- concentrations at almost all sites (Table S2) suggesting potential uncertainties in NH_3 emissions and their seasonal variability. Other potential reasons for the over-prediction of NO_3^- could be related to uncertainties in removal process of HNO_3 as well as dry deposition velocity of NH_3. Substantial over-predictions were found at the higher altitude site of Montseny and Puy de Dôme when compared with first model layer concentrations (ca. 200 and 800 meters a.s.l. respectively at these sites). These sites located at about 720 and 1465 meters a.s.l., are sometimes not within the PBLH during winter periods. At the Montseny site, the relatively coarse resolution of the model could also influence model performance since the site is located in a complex area about 50 km north-east of Barcelona (Pandolfi et al., 2014). Sulfate concentrations (SO_4^{2-}) were over-predicted at almost all sites and especially at Mace Head suggesting that long-range transport of SO_4^{2-} might be positively biased.

Modelled and observed hourly concentrations of NO_3^-, SO_4^{2-}, ammonium (NH_4^+) and OA at Payerne are reported in Fig. 4 for March 2009 together with meteorological parameters in Fig. S6. The model was able to reproduce the meteorological parameters very well for most of the time. The temperature was slightly under-predicted at both night and day-times (with a maximum of -2 °C) whereas both the monthly variation and the absolute values of wind speed and specific humidity were reproduced well with a few under-predictions of high wind-speed (6^{th} and 11^{th} of March and towards the end of the simulation). The model was able to capture the three NO_3^- and NH_4^+ peaks observed around the 7^{th}, 18^{th} and 23^{rd} of March with a general slight over-prediction throughout the whole period. Indeed, the under-prediction in temperature during day and night time could partially explain the over-prediction of the NO_3^- fraction with more NO_3^- partitioning to the aerosol phase which also apply to the other stations used in this study. An evaluation of modelled temperature at the European scale for the February-March 2009 period confirmed that the model systematically under-predicted the 2 meter surface temperature (Bessagnet et al., 2014). All the inorganic components were over-predicted during the first four days of March 2009 with a peak around the 3^{rd} of March,

indicating that the PBLH was probably not correctly reproduced by the model during this period. Although the temporal variation was captured, concentrations of OA were under-predicted throughout all the simulation (4.1 μg m^{-3} and 1.8 μg m^{-3} observed and modelled average concentrations). Analysis of the OA fraction is discussed in the next section.

3.3 Organic aerosols

3.3.1 Sensitivity of OA to the VBS scheme

In this section, effects of different parameterizations of the organic aerosol module on the modelled OA concentrations are discussed. The scatter plots in Fig. 5 show a comparison of daily average OA concentrations against the same AMS measurements as in Table 3 during February-March 2009. Statistics for each scenario are reported in Table 4. When the semi-volatile dynamics of primary organic aerosol is not taken into account (scenario NOVBS), the model under-predicts OA concentrations (MFB: -66%) with an observed and modelled average concentrations of 3.0 μg m^{-3} and 1.2 μg m^{-3} respectively. In the VBS_ROB scenario POA emissions are allowed to evaporate following the volatility distribution proposed by Robinson et al. (2007) and to undergo chemical oxidation. In this case modelled OA concentrations decrease by about 42% with respect to NOVBS, predicting an average OA concentration of 0.7 μg m^{-3}. On the other hand, the VBS_BC scenario improves the OA model performance increasing the OA concentrations by about 42% with respect to NOVBS. Predicted OA concentrations are found to be 1.7 μg m^{-3} on average (MFB: -47%). Similar behavior during winter periods was also shown in recent studies where the same VBS scheme was applied in the U.S. domain (Koo et al., 2014). Figure 6 shows the modelled total OA concentration over Europe using NOVBS, VBS_ROB and VBS_BC scenarios. The model predicts high OA values in the Eastern part of the domain as well as over Portugal, France and the Po Valley (VBS_BC). Some hot-spots around large urban areas are also visible, i.e., Paris and Moscow. Higher OA concentrations in the southern part of the domain are observed in the VBS_BC case, likely because of higher temperature and more OH radicals available in that part of the domain leading to an increase in the total organic mass upon reaction with organic vapours. This is in line with the results of Fountoukis et al. (2014) for the February-March 2009 period even though their study predicts lower concentration over the Po valley. Even though model input data and parameterizations are not the same, the VBS_BC case in particularly, uses a very similar volatility distribution as in Fountoukis et al. (2014). Our study

predicts relatively lower OA concentrations (MFB: -0.47, MFE: 0.79) compared to those reported by Fountoukis et al. (2014) (MFB: 0.02, MFE: 0.68) for February-March 2009. Unlike Fountoukis et al. (2014) our study does not include fire emissions and marine organic aerosol which may partially explain the differences. Figure 7 shows hourly modelled and observed OA concentration at Payerne for March 2009 and June 2006. In March 2009 VBS_ROB results are lower than those in NOVBS whereas OA concentrations in VBS_BC case are higher (see Supplementary Fig. S8 and Table S3 for average concentrations and statistics). In June 2006, the OA mass in VBS_ROB is lower than those in NOVBS while VBS_BC predicts similar concentrations as the NOVBS scenario (2.4 μg m^{-3} and 2.6 μg m^{-3}, respectively, Fig. S9 and Table S4). It has to be noted that the NOVBS scenario predicts slightly lower OA concentration for June 2006 in Payerne with respect to our previous application (Aksoyoglu et al., 2011), mainly because of a different biogenic model being used which yields lower monoterpene and sesquiterpene emissions. Since both BVOCs and BBOA-like emissions are highly uncertain, sensitivity tests with increased biogenic and anthropogenic emissions were performed and results discussed in the next section (3.3.2).

3.3.2 Sensitivity of OA to BBOA-like and BVOC emissions

Emissions of BVOCs compounds (i.e. monoterpenes, isoprene and sesquiterpenes) were doubled in scenario VBS_BC_2xBVOC, whilst primary organic aerosol emissions from SNAP2 and SNAP10 (BBOA-like) were doubled in scenarios VBS_BC_2xBBOA, with other emissions and processes represented as in VBS_BC. Figure 8 shows modelled and observed OA daily average concentrations for the VBS_BC, VBS_BC_2xBVOC and VBS_BC_2xBBOA scenarios across the sites. Statistics for each scenario are reported in Table 5. Increasing biogenic emissions by a factor of two during February-March 2009 resulted in almost no change in the predicted total OA (1.7 μg m^{-3} and 1.8 μg m^{-3} for the VBS_BC and VBS_BC_2xBVOC scenarios, respectively). On the other hand, doubling the BBOA-like emissions (VBS_BC_2xBBOA) during the same period strongly increased the predicted OA mass (up to 2.8 μg m^{-3} on average). As a result the mean fractional bias decreased further, from -47% to -12% averaged across the sites. This could eventually confirm other studies where substantial under-predictions in residential wood burning emissions were underlined (e.g., Bergström et al., 2012). A few points above the 2:1 lines in VBS_BC_2xBBOA mainly belong to the sites of Montseny, Puy de Dôme and Helsinki.

During winter periods, it is likely that elevated stations such Montseny and Puy de Dôme are most of the time above the PBLH, as suggested by previous studies for Puy de Dôme (Freney et al., 2011), whereas model concentrations are extracted from the first layer of the model. In Helsinki, BBOA emissions seem to be overestimated or the dispersion underestimated in the model.

Comparison with a warmer period in June 2006 is reported as well for Payerne where AMS measurements were also available (Fig.9). In February-March 2009 increasing BBOA-like emissions (VBS_BC_2xBBOA) reduced the fractional bias from -85% in VBS_BC to -37% (Table S3) with an over-prediction occurring during 1-5 of March (Fig. 9, upper panel). As already discussed in Section 3.2, it is likely that the vertical mixing processes were not correctly represented by the model since also the inorganic components were over-predicted for the same period. Almost no change in the predicted OA mass was found when biogenic emissions were doubled (scenario VBS_BC_2xBVOC) (Fig. 9, upper panel) due to lower BVOCs emission during winter periods. Increasing BVOCs emissions in June 2006 increased the predicted OA mass at Payerne site especially during the 12-16 June and towards the end of the simulation period, where higher concentrations and temperature (Fig. S7) were also observed (Fig. 9, lower panel). In contrast, similar OA concentrations were predicted in Payerne for VBS_BC and VBS_BC_2xBBOA during June 2006 (with averages of 2.4 μg m^{-3} and 2.8 μg m^{-3} respectively). This is in line with a very recent source apportionment study based on ACSM (aerosol chemical speciation monitor) measurements performed in Zürich for 13 months (February 2011 - February 2012) which revealed substantial differences between the winter (February-March) and summer (June-August) f_{44} / f_{43} space (organic mass fraction measured at mass to charge ratio 44 and 43) indicating that summer OOA (oxygenated organic aerosol) is strongly influenced by biogenic emission and winter OOA by biomass burning emission (Canonaco et al., 2015). Increased OA concentrations at Payerne in June 2006 with increased biogenic emissions were also found in other modelling studies. Bergström et al. (2012) used the VBS framework with different assumptions regarding aging processes and compared the model results for June 2006 with the AMS results at Payerne. In their study the total OA was found to be under-predicted with lower bias observed when aging processes were taken into account and biogenic emissions were increased by a factor of 3. Even though their model differs from ours in various aspects (number of volatility bins, aging processes parameterization and input data) in two of their scenario without aging of biogenic SOA Bergström et al. (2012) predicted an average OA concentration ranging from

2.6 μg m^{-3} to 3.4 μg m^{-3} which is similar to our base case VBS_BC and VBS_BC_2xBVOC scenario (2.4 μg m^{-3} and 3.4 μg m^{-3}, respectively, Table S4).

3.3.3 OA components in summer and winter

Comparisons of the primary and secondary organic fraction at the rural site of Payerne during summer (June 2006) and winter (February-March 2009) periods are reported in Figure 10. During the winter period the VBS scheme better reproduced the primary and secondary organic aerosol components compared to the NOVBS case. In particular, For the VBS_ROB base case, total OA concentrations were lower compared to the NOVBS case, consistent with the study of Woody et al. (2016) where the same VBS scheme was applied to the US domain. The total OA concentrations in the base case (VBS_BC) and in the scenario with increased biomass burning emissions (VBS_BC_2xBBOA) were higher compared to NOVBS case, even though SOA and POA fractions were not correctly reproduced. Higher contribution from the primary fraction during winter periods was also predicted by the study of Koo et al., 2014 which deployed the same VBS scheme. Eventually, this might indicate that biomass burning precursors might be missing in this study, or that the oxidation pathways of primary organic material need to be improved in the model (up to 86% of the reacted primary organic material is still allocated in the primary set as oxidation proceeds, directly increasing the POA fraction).

Different behavior was observed for the summer period where the larger contribution of SOA to the total OA retrieved from measurements is also reproduced by the model, even though the total OA concentration was still underestimated. These results for summer are also in line with the study of Koo et al. (2014) for summer periods in the US domain using the same VBS scheme.

4 Conclusions

A modelling study using the regional air quality model CAMx with VBS (Volatility Basis Set) scheme was performed for the first time in Europe within the EURODELTA-III model intercomparison exercise. An evaluation for the main gas phase species and $PM_{2.5}$ for four different periods was performed using the European air quality database Airbase as well as AMS (Aerosol Mass Spectrometer) measurements. The period in February-March 2009 was further analyzed in more detail using different assumptions regarding the volatility of emitted

organic aerosol and emissions of precursor. The main findings of this study are summarized below:

- Although total $PM_{2.5}$ mass concentrations and its variations were well reproduced by the model in all four periods, comparisons with AMS measurements for the February–March 2009 period revealed that the good agreement between model and measurements was most of the time due to overestimation of the inorganic fraction, especially NO_3^-, and underestimation of OA. Sensitivity tests with reduced NH_3 emissions generally reduced the positive bias in NO_3^- suggesting potential uncertainties in NH_3 emissions and their seasonal variability.

- In general, for all the four periods, the model under-predicted NO_2 and CO concentrations. On the other hand, O_3 was found to be over-predicted likely because of insufficient NO_x to undergo titration during night-time chemistry or not well captured vertical mixing processes and concentrations at the boundaries. SO_2 was over-predicted presumably mainly because of uncertainties in high stack point sources representation in the model or too low deposition processes.

- Including evaporation and oxidation processes of primary organic particles with the volatility distribution proposed by Robinson et al. (2007) lowered the modelled OA mass both in winter and summer periods. On the other hand, the adjustment of the scheme by Robinson et al. (2007) suggested by Shrivastava et al. (2011) and Tsimpidi et al. (2010) brings model and observations into better agreement by reducing the negative bias for OA by about 29% (MFB) in winter.

- Sensitivity tests with increased BVOCs and BBOA-like emissions suggested that emissions from residential heating represent an important contributor to total OA during winter periods (February-March 2009). The model under-predicted the winter OA concentrations (MFB -47% for base case VBS_BC) more than gas phase pollutants e.g. NO_2 (Table 2). Eventually, increasing BBOA-like emissions by a factor of 2 brought model and observation to a reasonably good agreement even though the model still under-predicts the OA fraction (-12% MFB). This underlines the necessity to better constrain emission inventories with a focus on residential heating. Also the implementation of the VBS scheme for domestic wood burning, which substantially influences both the primary and secondary organic aerosol, should be evaluated.

- A summer period was simulated as well and results were compared at Payerne. In June 2006, the current VBS implementation could not explain the discrepancy between modelled and observed OA. During this period the difference between the model and measurements is likely to be related to BVOCs emissions which are uncertain and difficult to constrain with measurements. In this case the model was sensitive to an increase in biogenic emissions especially during periods with higher temperature and OA concentrations. The latter could confirm the importance of BVOC precursors in summer in Payerne and the way to correctly represent their evolution in the atmosphere.

Acknowledgements

We thank the EURODELTA-III modelling community, especially INERIS for providing various model input data. We are grateful to ENVIRON for providing the CAMx-VBS code before its public release. Calculations of land use data were performed with the Swiss National Supercomputing Centre (CSCS). We thank D. Oderbolz for developing the CAMxRunner framework to ensure reproducibility and data quality among the simulations and sensitivity tests. We thank M. Tinguely for the visualization software. We also thank G. Pirovano for helping with the pre-processing of Airbase data. This study was financially supported by the Swiss Federal Office of Environment (FOEN). JLJ was supported by NSF AGS-1360834 and EPA STAR 83587701-0. We thank D.A. Day for analysis on the DAURE dataset. Erik Swietlicki for the Vavihill dataset, A. Kiendler-Scharr for Cabauw AMS data, Evelyn Freney for the Puy de Dôme dataset.

References

Aksoyoglu, S., Keller, J., Barmpadimos, I., Oderbolz, D., Lanz, V. A., Prévôt, A. S. H., and Baltensperger, U.: Aerosol modelling in ˆ Europe with a focus on Switzerland during summer and winter episodes, Atmos. Chem. Phys., 11, 7355–7373, doi:10.5194/acp- 11-7355-2011, 2011.

Athanasopoulou, E., Vogel, H., Vogel, B., Tsimpidi, A. P., Pandis, S. N., Knote, C., and Fountoukis, C.: Modeling the meteorological and chemical effects of secondary organic aerosols during an EUCAARI campaign, Atmos. Chem. Phys., 13, 625-645, doi:10.5194/acp-13-625-2013, 2013.

Appel, K.W., Gilliam, R.C., Davis, N., Zubrow, A., and Howard, S.C.: Overview of the Atmospheric Model Evaluation Tool (AMET) v1.1 for evaluating meteorological and air quality models, Environ. Modell. Softw., 26, 4, 434-443, 2011.

Benedetti, A., Morcrette, J.-J., Boucher, O., Dethof, A., Engelen, R.J., Fisher, M., Flentje, H., Huneeus, N., Jones, L., Kaiser, J.W., Kinne, S., Mangold, A., Razinger, M., Simmons, A.J., Suttie, M.: Aerosol analysis and forecast in the European Centre for Medium-Range Weather Forecasts Integrated Forecast System: 2. data assimilation. J. Geophys. Res. 114, D13205, 2009.

Bergström, R., Denier van der Gon, H. A. C., Prévôt, A. S. H., Yttri, K. E., and Simpson, D.: Modelling of organic aerosols over Europe (2002–2007) using a volatility basis set (VBS) framework: application of different assumptions regarding the formation of secondary organic aerosol, Atmos. Chem. Phys., 12, 8499–8527, doi:10.5194/acp-12-8499-2012, 2012.

Bessagnet, B., Colette, A., Meleux, F., Rouïl, L., Ung, A., Favez, O., Cuvelier, C., Thunis, P., Tsyro, S., Stern, R., Manders, A., Kranenburg, R., Aulinger, A., Bieser, J., Mircea, M., Briganti, G., Cappelletti, A., Calori, G., Finardi, S., Silibello, C., Ciarelli, G., Aksoyoglu, S.,

Prévôt, A., Pay, M.-T., Baldasano, J. M., García Vivanco, M., Garrido, J. L., Palomino, I., Martín, F., Pirovano, G., Roberts, P., Gonzalez, L., White, L., Menut, L., Dupont, J.C., Carnevale, C., and Pederzoli, A.: The EURODELTA III exercise “Model evaluation with observations issued from the 2009 EMEP intensive period and standard measurements in Feb/Mar 2009", MSC-W Technical Report, 2014.

Bessagnet, B., Pirovano, G., Mircea, M., Cuvelier, C., Aulinger, A., Calori, G., Ciarelli, G., Manders, A., Stern, R., Tsyro, S., García Vivanco, M., Thunis, P., Pay, M.-T., Colette, A., Couvidat, F., Meleux, F., Rouïl, L., Ung, A., Aksoyoglu, S., Baldasano, J. M., Bieser, J., Briganti, G., Cappelletti, A., D'Isodoro, M., Finardi, S., Kranenburg, R., Silibello, C., Carnevale, C., Aas, W., Dupont, J.-C., Fagerli, H., Gonzalez, L., Menut, L., Prévôt, A. S. H., Roberts, P., and White, L.: Presentation of the EURODELTA III inter-comparison exercise – Evaluation of the chemistry transport models performance on criteria pollutants and joint analysis with meteorology, Atmos. Chem. Phys. Discuss., doi:10.5194/acp-2015-736, 2016.

Boylan, J. W. and Russell, A. G.: PM and light extinction model performance metrics, goals, and criteria for three-dimensional air quality models, Atmos. Environ., 40, 4946–4959, 2006.

Canonaco, F., Slowik, J. G., Baltensperger, U., and Prévôt, A. S. H.: Seasonal differences in oxygenated organic aerosol composition: implications for emissions sources and factor analysis, Atmos. Chem. Phys., 15, 6993-7002, doi:10.5194/acp-15-6993-2015, 2015.

Cappa, C. D. and Jimenez, J. L.: Quantitative estimates of the volatility of ambient organic aerosol, Atmos. Chem. Phys., 10, 5409-5424, doi:10.5194/acp-10-5409-2010, 2010.

Chang, J. S., Brost, R. A., Isaksen, I. S. A., Madronich, S., Middleton, P., Stockwell, W. R., and Walcek, C. J.: A three-dimensional eulerian acid deposition model : Physical concepts and formulation, J. Geophys. Res., 92, 14681–14700, 1987.

646 Crippa, M., Canonaco, F., Lanz, V. A., Äijälä, M., Allan, J. D., Carbone, S., Capes, G.,
647 Ceburnis, D., Dall'Osto, M., Day, D. A., DeCarlo, P. F., Ehn, M., Eriksson, A., Freney, E.,
648 Hildebrandt Ruiz, L., Hillamo, R., Jimenez, J. L., Junninen, H., Kiendler-Scharr, A.,
649 Kortelainen, A.-M., Kulmala, M., Laaksonen, A., Mensah, A. A., Mohr, C., Nemitz, E.,
650 O'Dowd, C., Ovadnevaite, J., Pandis, S. N., Petäjä, T., Poulain, L., Saarikoski, S., Sellegri,
651 K., Swietlicki, E., Tiitta, P., Worsnop, D. R., Baltensperger, U., and Prévôt, A. S. H.: Organic
652 aerosol components derived from 25 AMS data sets across Europe using a consistent ME-2
653 based source apportionment approach, Atmos. Chem. Phys., 14, 6159– 6176,
654 doi:10.5194/acp-14-6159-2014, 2014.

655

656 Donahue, N., Robinson, A., Stanier, C., and Pandis, S.: Coupled Partitioning, Dilution, and
657 Chemical Aging of Semivolatile Organics, Environ. Sci. Technol., 40, 2635–2643, 2006.

658

659 Donahue, N. M., Epstein, S. A., Pandis, S. N., and Robinson, A. L.: A two-dimensional
660 volatility basis set: 1. organic-aerosol mixing thermodynamics, Atmos. Chem. Phys., 11,
661 3303–3318, doi:10.5194/acp-11-3303-2011, 2011.

662

663 Donahue, N. M., Henry, K. M., Mentel, T. F., Kiendler-Scharr, A., Spindler, C., Bohn, B.,
664 Brauers, T., Dorn, H. P., Fuchs, H., Tillmann, R., Wahner, A., Saathoff, H., Naumann, K. H.,
665 Mohler, O., Leisner, T., Muller, L., Reinnig, M. C., Hoffmann, T., Salo, K., Hallquist, M.,
666 Frosch, M., Bilde, M., Tritscher, T., Barmet, P., Praplan, A. P., DeCarlo, P. F., Dommen, J.,
667 Prevot, A. S. H., and Baltensperger, U.: Aging of biogenic secondary organic aerosol via gas-
668 phase OH radical reactions, P. Natl. Acad. Sci., 109, 13503–13508,
669 doi:10.1073/pnas.1115186109, 2012a.

670

671 Donahue, N. M., Kroll, J. H., Pandis, S. N., and Robinson, A. L.: A two-dimensional
672 volatility basis set – Part 2: Diagnostics of organic-aerosol evolution, Atmos. Chem. Phys.,
673 12, 615–634, doi:10.5194/acp-12-615-2012, 2012b.

674

675 ETC/ACC, Improvement of classifications European monitoring stations for AirBase - A
676 quality control, Technical Paper 2004/7.
677
678 Environ: User's Guide, Comprehensive Air Quality Model with Extensions (CAMx), Version
679 5.40, Environ International Corporation, California, 2011.
680
681 Freney, E. J., Sellegri, K., Canonaco, F., Boulon, J., Hervo, M., Weigel, R., Pichon, J. M.,
682 Colomb, A., Prévôt, A. S. H., and Laj, P.: Seasonal variations in aerosol particle composition
683 at the puy-de-Dôme research station in France, Atmos. Chem. Phys., 11, 13047-13059,
684 doi:10.5194/acp-11-13047-2011, 2011.
685 Fountoukis, C., Racherla, P. N., Denier van der Gon, H. A. C., Polymeneas, P.,
686 Charalampidis, P. E., Pilinis, C., Wiedensohler, A., Dall'Osto, M., O'Dowd, C., and Pandis,
687 S. N.: Evaluation of a three-dimensional chemical transport model (PMCAMx) in the
688 European domain during the EUCAARI May 2008 campaign, Atmos. Chem. Phys., 11,
689 10331–10347, doi:10.5194/acp-11-10331-2011, 2011.
690
691 Fountoukis, C., Megaritis, A. G., Skyllakou, K., Charalampidis, P. E., Pilinis, C., Denier van
692 der Gon, H. A. C., Crippa, M., Canonaco, F., Mohr, C., Prévôt, A. S. H., Allan, J. D., Poulain,
693 L., Petäjä, T., Tiitta, P., Carbone, S., Kiendler-Scharr, A., Nemitz, E., O'Dowd, C., Swietlicki,
694 E., and Pandis, S. N.: Organic aerosol concentration and composition over Europe: insights
695 from comparison of regional model predictions with aerosol mass spectrometer factor
696 analysis, Atmos. Chem. Phys., 14, 9061-9076, doi:10.5194/acp-14-9061-2014, 2014.
697
698 Guenther, A. B., Jiang, X., Heald, C. L., Sakulyanontvittaya, T., Duhl, T., Emmons, L. K.,
699 and Wang, X.: The Model of Emissions of Gases and Aerosols from Nature version 2.1
700 (MEGAN2.1): an extended and updated framework for modeling biogenic emissions, Geosci.
701 Model Dev., 5, 1471–1492, doi:10.5194/gmd-5- 1471-2012, 2012.
702
703 Hallquist, M., Wenger, J. C., Baltensperger, U., Rudich, Y., Simpson, D., Claeys, M.,
704 Dommen, J., Donahue, N. M., George, C., Goldstein, A. H., Hamilton, J. F., Herrmann, H.,

Hoffmann, T., Iinuma, Y., Jang, M., Jenkin, M. E., Jimenez, J. L., Kiendler-Scharr, A., Maenhaut, W., McFiggans, G., Mentel, Th. F., Monod, A., Prévôt, A. S. H., Seinfeld, J. H., Surratt, J. D., Szmigielski, R., and Wildt, J.: The formation, properties and impact of secondary organic aerosol: current and emerging issues, Atmos. Chem. Phys., 9, 5155–5236, doi:10.5194/acp-9-5155- 2009, 2009.

Hodzic, A., Jimenez, J. L., Madronich, S., Canagaratna, M. R., DeCarlo, P. F., Kleinman, L., and Fast, J.: Modeling organic aerosols in a megacity: potential contribution of semi-volatile and intermediate volatility primary organic compounds to secondary organic aerosol formation, Atmos. Chem. Phys., 10, 5491-5514, doi:10.5194/acp-10-5491-2010, 2010.

Inness, A., Baier, F., Benedetti, A., Bouarar, I., Chabrillat, S., Clark, H., Clerbaux, C., Coheur, P., Engelen, R. J., Errera, Q., Flemming, J., George, M., Granier, C., Hadji-Lazaro, J., Huijnen, V., Hurtmans, D., Jones, L., Kaiser, J. W., Kapsomenakis, J., Lefever, K., Leitão, J., Razinger, M., Richter, A., Schultz, M. G., Simmons, A. J., Suttie, M., Stein, O., Thépaut, J.-N., Thouret, V., Vrekoussis, M., Zerefos, C., and the MACC team: The MACC reanalysis: an 8 yr data set of atmospheric composition, Atmos. Chem. Phys., 13, 4073-4109, doi:10.5194/acp-13-4073-2013, 2013.

Jo, D. S., Park, R. J., Kim, M. J., and Spracklen, D. V.: Effects of chemical aging on global secondary organic aerosol using the volatility basis set approach, Atmos. Environ., 81, 230–244, doi:10.1016/j.atmosenv.2013.08.055, 2013.

Knote, C., Brunner, D., Vogel, H., Allan, J., Asmi, A., Äijälä, M., Carbone, S., van der Gon, H. D., Jimenez, J. L., Kiendler-Scharr, A., Mohr, C., Poulain, L., Prévôt, A. S. H., Swietlicki, E., and Vogel, B.: Towards an online-coupled chemistry-climate model: evaluation of trace gases and aerosols in COSMO-ART, Geosci. Model Dev., 4, 1077-1102, doi:10.5194/gmd-4-1077-2011, 2011.

Koo, B., Knipping, E., Yarwood, G.: 1.5-Dimensional volatility basis set approach for modeling organic aerosol in CAMx and CMAQ, Atmos Environ., 95: 158-164., 2014.

735

736 Kuenen, J. J. P., Denier van der Gon, H. A. C., Visschedijk, A., Van der Brugh, H., and Van
737 Gijlswijk, R.: MACC European emission inventory for the years 2003–2007, TNO report
738 TNO- 060-UT-2011-00588, TNO, Utrecht, 2011.

739

740 Kulmala, M., Asmi, A., Lappalainen, H. K., Carslaw, K. S., Pöschl, U., Baltensperger, U.,
741 Hov, Ø., Brenquier, J.-L., Pandis, S. N., Facchini, M. C., Hansson, H.-C., Wiedensohler, A.,
742 and O'Dowd, C. D.: Introduction: European Integrated Project on Aerosol Cloud Climate and
743 Air Quality interactions (EUCAARI) – integrating aerosol research from nano to global
744 scales, Atmos. Chem. Phys., 9, 2825–2841, doi:10.5194/acp-9-2825-2009, 2009.

745 Kulmala, M., Asmi, A., Lappalainen, H. K., Baltensperger, U., Brenguier, J.-L., Facchini, M.
746 C., Hansson, H.-C., Hov, Ø., O'Dowd, C. D., Pöschl, U., Wiedensohler, A., Boers, R.,
747 Boucher, O., de Leeuw, G., Denier van der Gon, H. A. C., Feichter, J., Krejci, R., Laj, P.,
748 Lihavainen, H., Lohmann, U., McFiggans, G., Mentel, T., Pilinis, C., Riipinen, I., Schulz, M.,
749 Stohl, A., Swietlicki, E., Vignati, E., Alves, C., Amann, M., Ammann, M., Arabas, S., Artaxo,
750 P., Baars, H., Beddows, D. C. S., Bergström, R., Beukes, J. P., Bilde, M., Burkhart, J. F.,
751 Canonaco, F., Clegg, S. L., Coe, H., Crumeyrolle, S., D'Anna, B., Decesari, S., Gilardoni, S.,
752 Fischer, M., Fjaeraa, A. M., Fountoukis, C., George, C., Gomes, L., Halloran, P., Hamburger,
753 T., Harrison, R. M., Herrmann, H., Hoffmann, T., Hoose, C., Hu, M., Hyvärinen, A., Hõrrak,
754 U., Iinuma, Y., Iversen, T., Josipovic, M., Kanakidou, M., Kiendler-Scharr, A., Kirkevåg, A.,
755 Kiss, G., Klimont, Z., Kolmonen, P., Komppula, M., Kristjánsson, J.-E., Laakso, L.,
756 Laaksonen, A., Labonnote, L., Lanz, V. A., Lehtinen, K. E. J., Rizzo, L. V., Makkonen, R.,
757 Manninen, H. E., McMeeking, G., Merikanto, J., Minikin, A., Mirme, S., Morgan, W. T.,
758 Nemitz, E., O'Donnell, D., Panwar, T. S., Pawlowska, H., Petzold, A., Pienaar, J. J., Pio, C.,
759 Plass-Duelmer, C., Prévôt, A. S. H., Pryor, S., Reddington, C. L., Roberts, G., Rosenfeld, D.,
760 Schwarz, J., Seland, Ø., Sellegri, K., Shen, X. J., Shiraiwa, M., Siebert, H., Sierau, B.,
761 Simpson, D., Sun, J. Y., Topping, D., Tunved, P., Vaattovaara, P., Vakkari, V., Veefkind, J.
762 P., Visschedijk, A., Vuollekoski, H., Vuolo, R., Wehner, B., Wildt, J., Woodward, S.,
763 Worsnop, D. R., van Zadelhoff, G.-J., Zardini, A. A., Zhang, K., van Zyl, P. G., Kerminen,
764 V.-M., S Carslaw, K., and Pandis, S. N.: General overview: European Integrated project on
765 Aerosol Cloud Climate and Air Quality interactions (EUCAARI) – integrating aerosol

766 research from nano to global scales, Atmos. Chem. Phys., 11, 13061–13143, doi:10.5194/acp-
767 11-13061-2011, 2011.

768

769 Lane, T. E., Donahue, N. M., and Pandis, S. N.: Simulating secondary organic aerosol
770 formation using the volatility basis-set approach in a chemical transport model, Atmos.
771 Environ., 42, 7439–7451, doi:10.1016/j.atmosenv.2008.06.026, 2008.

772

773 Langmann, B., Sellegri, K., and Freney, E.: Secondary organic aerosol formation during June
774 2010 in Central Europe: measurements and modelling studies with a mixed thermodynamic-
775 kinetic approach, Atmos. Chem. Phys., 14, 3831-3842, doi:10.5194/acp-14-3831-2014, 2014.

776 Li, Y. P., Elbern, H., Lu, K. D., Friese, E., Kiendler-Scharr, A., Mentel, Th. F., Wang, X. S.,
777 Wahner, A., and Zhang, Y. H.: Updated aerosol module and its application to simulate
778 secondary organic aerosols during IMPACT campaign May 2008, Atmos. Chem. Phys., 13,
779 6289-6304, doi:10.5194/acp-13-6289-2013, 2013.

780

781 Madronich, S.: The Tropospheric Visible Ultra-violet (TUV) model web page, National
782 Center for Atmospheric Research, Boulder, CO., http://www.acd.ucar.edu/TUV/, 2002.

783

784 Mensah, A. A., Holzinger, R., Otjes, R., Trimborn, A., Mentel, Th. F., ten Brink, H., Henzing,
785 B., and Kiendler-Scharr, A.: Aerosol chemical composition at Cabauw, The Netherlands as
786 observed in two intensive periods in May 2008 and March 2009, Atmos. Chem. Phys., 12,
787 4723-4742, doi:10.5194/acp-12-4723-2012, 2012.

788

789 Murphy, B. N. and Pandis, S. N.: Simulating the formation of semivolatile primary and
790 secondary organic aerosol in a regional chemical transport model, Environ. Sci. Technol., 43,
791 4722– 4728, 2009.

792

793 Murphy, B. N., Donahue, N. M., Fountoukis, C., Dall' Osto, M., O'Dowd, C., Kiendler-
794 Scharr, A., and Pandis, S. N.: Functionalization and fragmentation during ambient organic

795 aerosol aging: application of the 2-D volatility basis set to field studies, Atmos. Chem. Phys.,
796 12, 10797-10816, doi:10.5194/acp-12-10797-2012, 2012.
797
798 NASA/GSFC, Total ozone mapping spectrometer: http://toms.gsfc.
799 nasa.gov/ozone/ozone.html, 2005.
800
801 Nenes, A., Pandis, S. N., and Pilinis, C.: ISORROPIA: A new thermodynamic equilibrium
802 model for multiphase multicomponent inorganic aerosols, Aquatic Geochemistry, 4, 123–152,
803 1998.
804
805 Pandolfi, M., Querol, X., Alastuey, A., Jimenez, J.L., Jorba, O., Day, D., Ortega, A., Cubison,
806 M.J., Comerón, A., Sicard, M., Mohr, C., Prévôt, A.S.H., Minguillón, M.C., Pey, J.,
807 Baldasano, J.M., Burkhart, J.F., Seco, R., Peñuelas, J., Van Drooge, B.L., Artiñano, B., Di
808 Marco, C., Nemitz, E., Schallhart, S., Metzger, A., Hansel, A., Lorente, J., Ng, S., Jayne J.,
809 and Szidat, S.: Effects of sources and meteorology on particulate matter in the Western
810 Mediterranean Basin: an overview of the DAURE campaign, J. Geophys. Res. Atmos., 119
811 http://dx.doi.org/10.1002/2013JD021079, 2014.
812
813 Passant, N. R.: Speciation of UK emissions of non-methane volatile organic compounds,
814 AEA Technology, Culham, 289, 2002.
815
816 Robinson, A. L., Donahue, N. M., Shrivastava, M. K., Weitkamp, E. A., Sage, A. M.,
817 Grieshop, A. P., Lane, T. E., Pierce, J. R., and Pandis, S. N.: Rethinking Organic Aerosols:
818 Semivolatile Emissions and Photochemical Aging, Science, 315, 1259–1262,
819 doi:10.1126/science.1133061, 2007.
820
821 Shrivastava, M., Fast, J., Easter, R., Gustafson Jr., W. I., Zaveri, R. A., Jimenez, J. L., Saide,
822 P., and Hodzic, A.: Modeling organic aerosols in a megacity: comparison of simple and

823 complex representations of the volatility basis set approach, Atmos. Chem. Phys., 11, 6639–
824 6662, doi:10.5194/acp-11-6639-2011, 2011.

825

826 Solazzo, E., Bianconi, R., Pirovano, G., Matthias, V., Vautard, R., Moran, M. D., Appel, K.
827 W., Bessagnet, B., Brandt, J., Christensen, J. H., Chemel, C., Coll, I., Ferreira, J., Forkel, R.,
828 Francis, X. V., Grell, G., Grossi, P., Hansen, A. B., Miranda, A. I., Nopmongcol, U., Prank,
829 M., Sartelet, K. N., Schaap, M., Silver, J. D., Sokhi, R. S., Vira, J., Werhahn, J., Wolke, R.,
830 Yarwood, G., Zhang, J., Rao, S. T., and Galmarini, S.: Operational model evaluation for
831 particulate matter in Europe and North America in the context of AQMEII, Atmos. Environ.,
832 53, 75–92, doi:10.1016/j.atmosenv.2012.02.045, 2012a.

833

834 Starcrest Consulting Group, LLC, Starcrest Consulting Group, LLC.: Port-Wide Baseline Air
835 Emissions Inventory. Prepared for the Port of Los Angeles, California, 2004.

836

837 Steinbacher, M., Zellweger, C., Schwarzenbach, B., Bugmann, S., Buchmann, B., Ordóñez,
838 C., Prevot, A. S. H., and Hueglin, C.: Nitrogen Oxides Measurements at Rural Sites in
839 Switzerland: Bias of Conventional Measurement Techniques, J. Geophys. Res., 2007.

840

841 Strader, R., Lurmann, F., and Pandis, S. N.: Evaluation of secondary organic aerosol
842 formation in winter, Atmos. Environ., 33, 4849– 4863, 1999.

843

844 Tsigaridis, K., Daskalakis, N., Kanakidou, M., Adams, P. J., Artaxo, P., Bahadur, R.,
845 Balkanski, Y., Bauer, S. E., Bellouin, N., Benedetti, A., Bergman, T., Berntsen, T. K.,
846 Beukes, J. P., Bian, H., Carslaw, K. S., Chin, M., Curci, G., Diehl, T., Easter, R. C., Ghan, S.
847 J., Gong, S. L., Hodzic, A., Hoyle, C. R., Iversen, T., Jathar, S., Jimenez, J. L., Kaiser, J. W.,
848 Kirkevåg, A., Koch, D., Kokkola, H., Lee, Y. H, Lin, G., Liu, X., Luo, G., Ma, X., Mann, G.
849 W., Mihalopoulos, N., Morcrette, J.-J., Müller, J.-F., Myhre, G., Myriokefalitakis, S., Ng, N.
850 L., O'Donnell, D., Penner, J. E., Pozzoli, L., Pringle, K. J., Russell, L. M., Schulz, M., Sciare,
851 J., Seland, Ø., Shindell, D. T., Sillman, S., Skeie, R. B., Spracklen, D., Stavrakou, T.,
852 Steenrod, S. D., Takemura, T., Tiitta, P., Tilmes, S., Tost, H., van Noije, T., van Zyl, P. G.,

853 von Salzen, K., Yu, F., Wang, Z., Wang, Z., Zaveri, R. A., Zhang, H., Zhang, K., Zhang, Q.,
854 and Zhang, X.: The AeroCom evaluation and intercomparison of organic aerosol in global
855 models, Atmos. Chem. Phys., 14, 10845-10895, doi:10.5194/acp-14-10845-2014, 2014.

856

857 Tsimpidi, A. P., Karydis, V. A., Zavala, M., Lei, W., Molina, L., Ulbrich, I. M., Jimenez, J.
858 L., and Pandis, S. N.: Evaluation of the volatility basis-set approach for the simulation of
859 organic aerosol formation in the Mexico City metropolitan area, Atmos. Chem. Phys., 10,
860 525-546, doi:10.5194/acp-10-525-2010, 2010.

861

862 Tørseth, K., Aas, W., Breivik, K., Fjæraa, A. M., Fiebig, M., Hjellbrekke, A. G., Lund Myhre,
863 C., Solberg, S., and Yttri, K. E.: Introduction to the European Monitoring and Evaluation
864 Programme (EMEP) and observed atmospheric composition change during 1972–2009,
865 Atmos. Chem. Phys., 12, 5447–5481, doi:10.5194/acp-12-5447-2012, 2012.

866

867 Vestreng, V., Myhre, G., Fagerli, H., Reis, S., and Tarrasón, L.: Twenty-five years of
868 continuous sulphur dioxide emission reduction in Europe, Atmos. Chem. Phys., 7, 3663-3681,
869 doi:10.5194/acp-7-3663-2007, 2007.

870

871 Vaughan, A.R., Lee, J.D., Misztal, P.K., Metzger, S., Shaw, M.D., Lewis, A.C., Purvis, R.M.,
872 Carslaw, D.C., Goldstein, A.H., Hewitt, C.N., Davison, B., Beevers, S.D., Karl, T.G.,
873 Spatially resolved flux measurements of NOx from London suggest significantly higher
874 emissions than predicted by inventories. Faraday Discuss. doi:10.1039/C5FD00170F, 2016

875

876 Villena, G., Bejan, I., Kurtenbach, R., Wiesen, P., and Kleffmann, J.: Interferences of
877 commercial NO_2 instruments in the urban atmosphere and in a smog chamber, Atmos. Meas.
878 Tech., 5, 149-159, doi:10.5194/amt-5-149-2012, 2012.

879 WHO, Burden of disease from Ambient Air Pollution for 2012 - Summary of results, 2014a.

880

881 Yarwood, G., Rao, S., Yocke, M., and Whitten, G. Z.: Updates to the Carbon Bond Chemical
882 Mechanism: CB05 Yocke & Company, Novato, CA 94945RT-04-00675, 2005.
883
884 Zhang, L., Brook, J. R., and Vet, R.: A revised parameterization for gaseous dry deposition in
885 air-quality models, Atmos. Chem. Phys., 3, 2067–2082, doi:10.5194/acp-3-2067-2003, 2003.
886
887 Zhang, Q. J., Beekmann, M., Drewnick, F., Freutel, F., Schneider, J., Crippa, M., Prevot, A.
888 S. H., Baltensperger, U., Poulain, L., Wiedensohler, A., Sciare, J., Gros, V., Borbon, A.,
889 Colomb, A., Michoud, V., Doussin, J.-F., Denier van der Gon, H. A. C., Haeffelin, M.,
890 Dupont, J.-C., Siour, G., Petetin, H., Bessagnet, B., Pandis, S. N., Hodzic, A., Sanchez, O.,
891 Honoré, C., and Perrussel, O.: Formation of organic aerosol in the Paris region during the
892 MEGAPOLI summer campaign: evaluation of the volatility-basis-set approach within the
893 CHIMERE model, Atmos. Chem. Phys., 13, 5767-5790, doi:10.5194/acp-13-5767-2013,
894 2013.
895

5 Figures and Tables

Table 1. Volatility distributions used for different scenarios.

Scenarios	POA emission sources	Emission fraction for volatility bin with C* of				
		0	1	10	100	1000
NOVBS (non-volatile CAMxv5.40)	HOA-like	1.00	-	-	-	-
	BBOA-like	1.00				
VBS_ROB (Robinson et al., 2007)	HOA-like	0.09	0.09	0.14	0.18	0.5
	BBOA-like	0.09	0.09	0.14	0.18	0.5
VBS_BC (Tsimpidi et al., 2010 and Shrivastava et al., 2011)	HOA-like	0.40	0.26	0.40	0.51	1.43
	BBOA-like	0.27	0.27	0.42	0.54	1.50

900 Table 2. Model gas phase and $PM_{2.5}$ performance for the EDIII field campaigns (base case
901 VBS_BC).

Species	Number of sites	Observed mean (ppb) ($\mu g\ m^{-3}$ for $PM_{2.5}$)	Modelled mean (ppb) ($\mu g\ m^{-3}$ for $PM_{2.5}$)	MB (ppb) ($\mu g\ m^{-3}$ for $PM_{2.5}$)	ME (ppb) ($\mu g\ m^{-3}$ for $PM_{2.5}$)	MFB [-]	MFE [-]	r
June 2006								
CO	36	192.0	158.0	-34.2	80.7	-0.12	0.36	0.20
NO_2	320	4.1	2.3	-1.9	2.2	-0.54	0.68	0.55
O_3	460	42.3	51.2	8.9	10.8	0.21	0.24	0.57
$PM_{2.5}$	48	12.0	11.7	-0.3	4.5	-0.07	0.39	0.55
SO_2	263	1.0	1.2	0.2	0.7	0.14	0.67	0.52
Jan-Feb 2007								
CO	45	248.0	191.0	-57.8	107.0	-0.11	0.37	0.21
NO_2	337	6.5	4.4	-2.2	3.2	-0.28	0.57	0.68
O_3	455	23.5	35.8	12.3	12.6	0.48	0.49	0.61
$PM_{2.5}$	56	11.7	12.8	1.0	6.1	-0.04	0.56	0.69
SO_2	271	1.3	1.7	0.4	1.1	0.36	0.75	0.46
Sep-Oct 2008								
CO	53	208.0	136.0	-72.0	91.4	-0.31	0.48	0.27
NO_2	370	5.3	3.7	-1.7	2.5	-0.28	0.56	0.62
O_3	465	24.3	32.5	8.2	9.6	0.32	0.37	0.50
$PM_{2.5}$	90	13.0	14.1	1.0	5.7	<0.01	0.46	0.76
SO_2	256	0.9	1.1	0.2	0.8	0.25	0.74	0.37
Feb-Mar 2009								
CO	57	262.0	170.0	-91.6	119.0	-0.26	0.48	0.37
NO_2	380	6.0	3.9	-2.0	2.8	-0.33	0.56	0.61
O_3	488	32.7	33.0	0.2	7.1	0.02	0.23	0.55
$PM_{2.5}$	110	15.1	13.0	-2.1	6.4	-0.13	0.50	0.71
SO_2	257	1.0	1.3	0.3	0.9	0.23	0.76	0.45

902

903

904

905 Table 3. Statistical analysis of nitrate, ammonium, sulfate and organic aerosol in base case
906 (VBS_BC) for February-March 2009 at different AMS sites.

907

Site	Mean observed ($\mu g/m^3$)	Mean modelled ($\mu g/m^3$)	MB $\mu g\ m^{-3}$	ME $\mu g\ m^{-3}$	MFB [-]	MFE [-]
		NO_3^-				
Barcelona	3.6	5.8	2.19	3.98	0.35	0.98
Cabauw	2.2	6.7	4.49	4.58	0.85	1.01
Chilbolton	2.7	4.0	1.33	2.21	0.02	0.76
Helsinki	1.0	1.9	0.93	1.30	0.29	0.92
Hyytiälä	0.2	1.0	0.75	0.83	0.21	1.09
Mace Head	0.6	1.7	1.11	1.12	0.14	0.70
Melpitz	3.1	4.3	1.25	2.41	0.35	0.71
Montseny	3.1	5.9	2.83	4.31	0.38	1.00
Payerne	3.9	5.7	1.81	2.83	0.34	0.61
Puy de Dôme	0.9	2.7	1.81	2.17	1.13	1.30
Vavihill	2.8	3.7	0.89	2.17	0.14	0.78
		NH_4^+				
Barcelona	1.6	2.5	0.92	1.41	0.42	0.71
Cabauw	1.0	2.7	1.73	1.75	0.95	0.97
Chilbolton	1.3	2.0	0.68	1.02	0.39	0.61
Helsinki	0.8	1.3	0.52	0.59	0.51	0.60
Hyytiälä	0.4	0.8	0.43	0.48	0.55	0.70
Melpitz	1.4	2.1	0.72	1.11	0.45	0.69
Montseny	1.7	2.6	0.92	1.58	0.39	0.74
Payerne	1.7	2.5	0.80	1.15	0.36	0.56
Puy de Dôme	0.7	1.2	0.51	0.87	0.83	1.07
Vavihill	1.6	1.9	0.38	0.90	0.17	0.56
		SO_4^{2-}				
Barcelona	2.7	2.3	-0.44	1.25	-0.19	0.48
Cabauw	1.0	2.1	1.13	1.34	0.73	0.85
Chilbolton	1.3	2.2	0.91	1.33	0.45	0.70
Helsinki	2.4	2.2	-0.24	0.92	-0.04	0.43
Hyytiälä	1.4	1.7	0.26	0.73	0.09	0.58
Mace Head	0.4	1.2	0.83	0.89	1.04	1.12
Melpitz	1.1	2.2	1.15	1.40	0.54	0.76
Montseny	1.4	2.3	0.97	1.19	0.55	0.64

Payerne	1.1	2.1	1.06	1.16	0.62	0.70
Puy de Dôme	0.4	1.1	0.77	0.82	1.14	1.19
Vavihill	1.6	2.3	0.73	1.05	0.18	0.54
		OA				
Barcelona	8.2	3.1	-5.11	5.15	-0.80	0.82
Cabauw	1.2	1.1	-0.14	0.53	-0.13	0.50
Chilbolton	2.4	0.7	-1.70	1.70	-1.09	1.10
Helsinki	2.7	2.9	0.26	1.64	0.08	0.62
Hyytiälä	1.3	1.0	-0.28	0.52	-0.48	0.60
Mace Head	0.8	0.4	-0.38	0.43	-0.29	0.70
Melpitz	1.5	0.5	-0.95	0.98	-0.94	0.97
Montseny	3.1	3.9	0.88	1.88	0.31	0.57
Payerne	4.1	1.8	-2.33	2.43	-0.85	0.90
Puy de Dôme	0.6	1.4	0.78	0.96	0.68	0.91
Vavihill	3.9	1.4	-2.53	2.53	-1.04	1.04

Table 4. Statistical analysis of OA for NOVBS, VBS_ROB and VBS_BC scenarios for the 11 AMS sites for February-March 2009.

Scenario	Mean observed OA ($\mu g\ m^{-3}$)	Mean modelled OA ($\mu g\ m^{3}$)	MB ($\mu g\ m^{-3}$)	ME ($\mu g\ m^{-3}$)	MFB [-]	MFE [-]
NOVBS	3.0	1.2	-1.8	2.0	−0.66	0.88
VBS_ROB	3.0	0.7	-2.3	2.4	−1.08	1.19
VBS_BC (base case)	3.0	1.7	-1.2	1.8	−0.47	0.79

Table 5. Statistical analysis of OA for VBS_BC, VBS_BC_2xBVOC and VBS_BC_2xBBOA scenarios for the 11 AMS sites for February-March 2009.

Scenario	Mean observed OA ($\mu g\ m^{-3}$)	Mean modelled OA ($\mu g\ m^{3}$)	MB ($\mu g\ m^{-3}$)	ME ($\mu g\ m^{-3}$)	MFB [-]	MFE [-]
VBS_BC (base case)	3.0	1.7	-1.2	1.8	−0.47	0.79
VBS_BC_2xBVOC	3.0	1.8	-1.2	1.8	−0.46	0.78
VBS_BC_2xBBOA	3.0	2.8	-0.1	1.9	−0.12	0.69

915

916

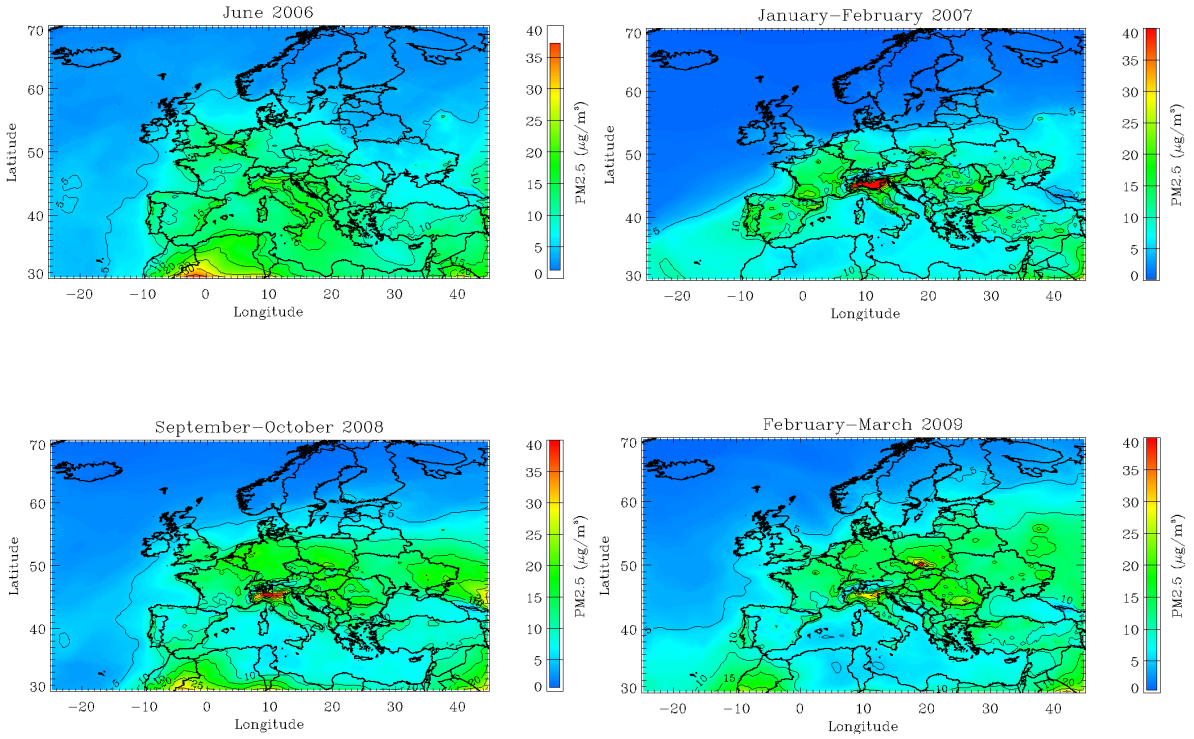

917

918

919 Figure 1. Modelled average $PM_{2.5}$ concentrations for June 2006, January-February 2007,
920 September-October 2008 and February-March 2009 (top to bottom) based on the base case
921 (VBS_BC). Note that the color scale was limited to maximum of 40 μg/m^3 to facilitate
922 comparison of the panels.

923

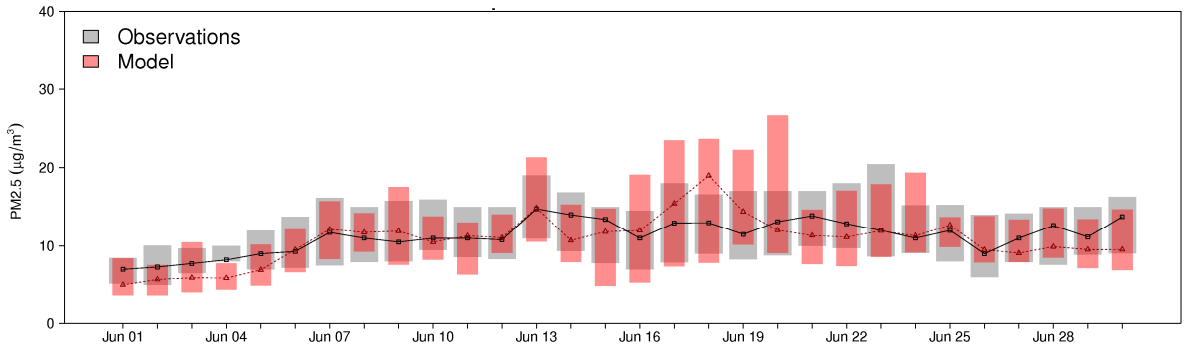

924

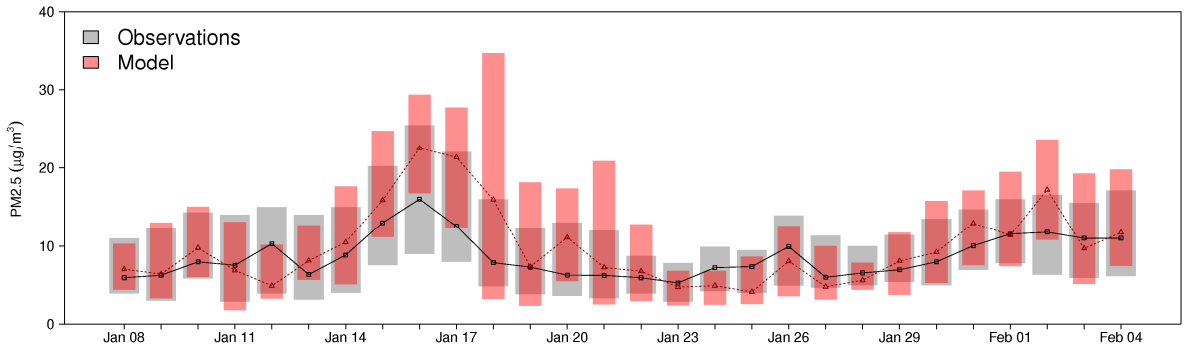

925

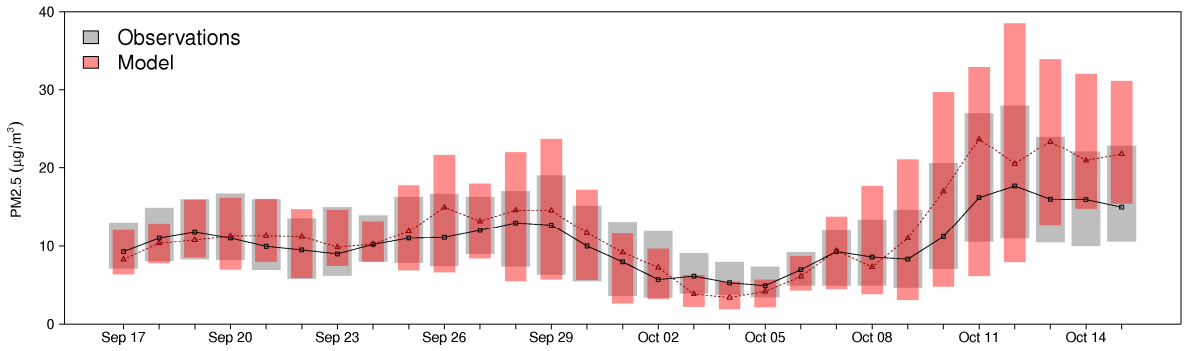

926

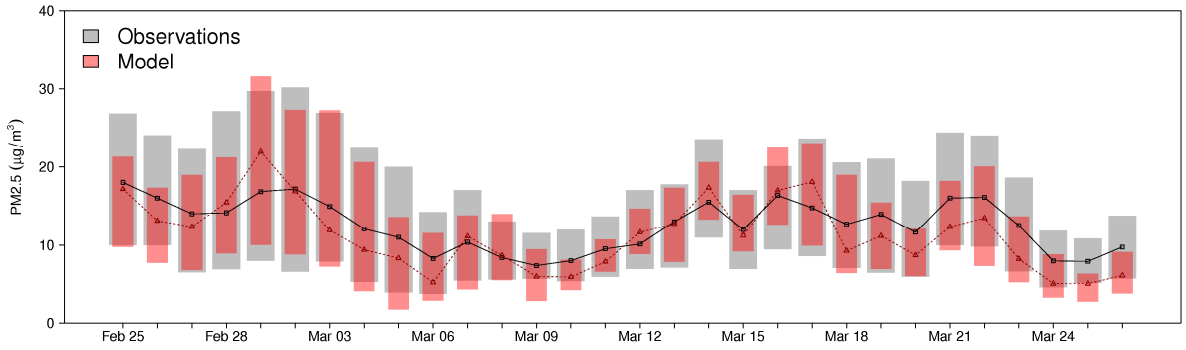

927

928 Figure 2. Comparison of modelled (red) and measured (grey) $PM_{2.5}$ concentrations at AirBase
929 rural background sites. The extent of the bars indicates the 25th and 75th percentile. The black

930 and red lines are observed and modelled median, respectively. The numbers of sites are 48,
931 56, 90, and 110 from top to down. Based on base case (VBS_BC).
932

933

934

935

936

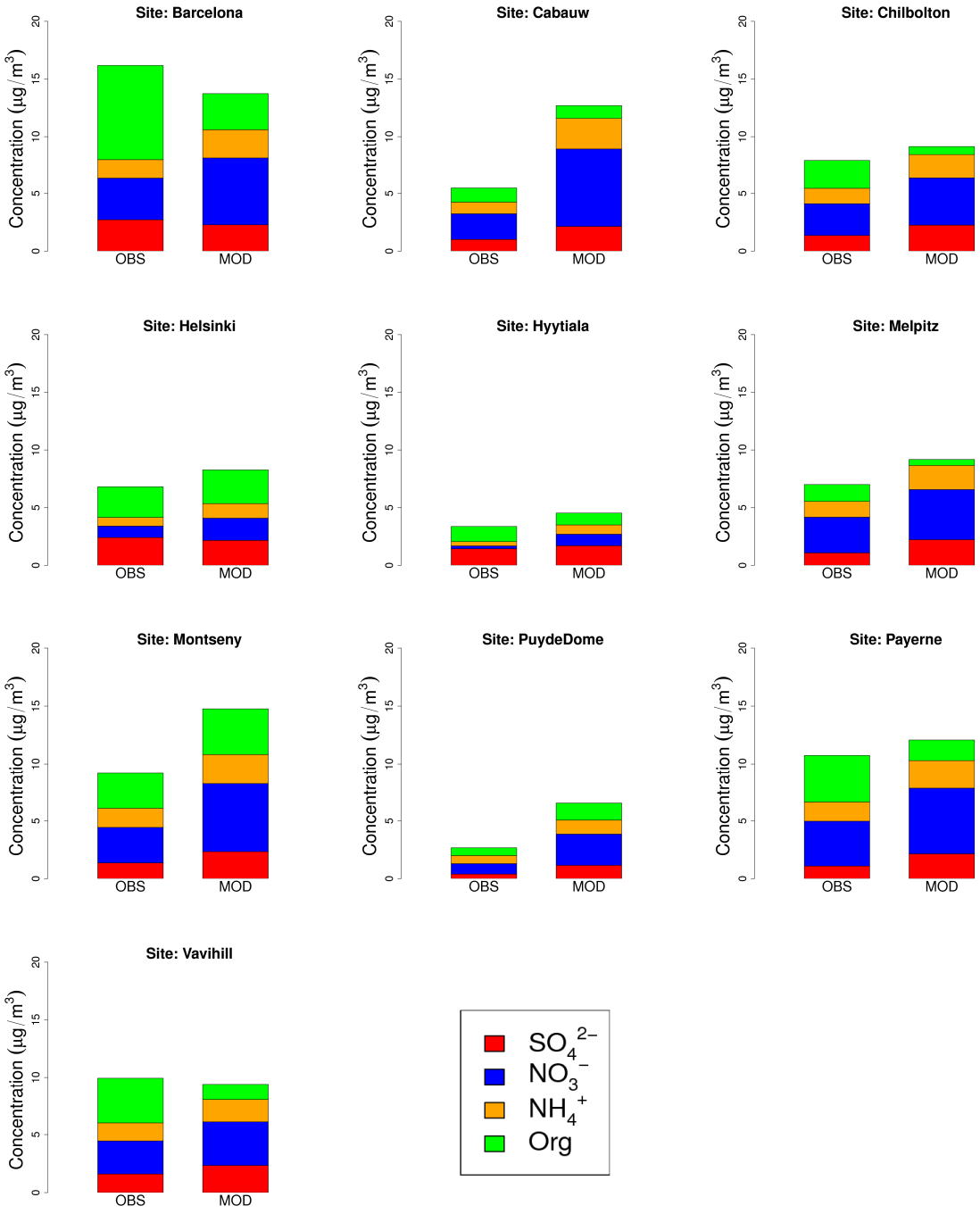

937 Figure 3. Comparison of observed (OBS) non-refractory PM_1 and modelled (MOD) non-
938 refractory $PM_{2.5}$ at 10 AMS sites in Europe during February-March 2009. Mace head is
939 reported only in Table 3 since the ammonium component is not available.

940

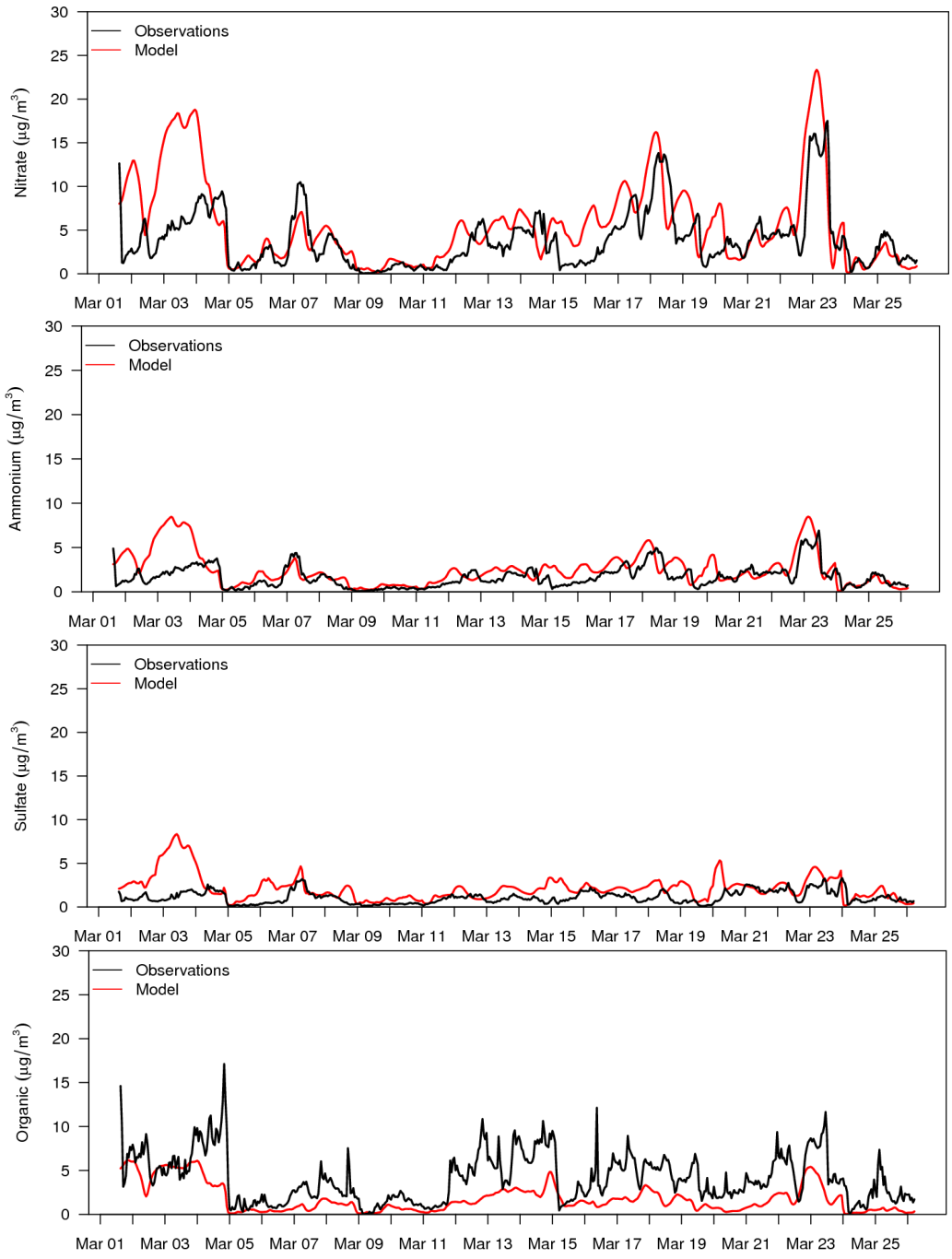

941

942

943

944

945 Figure 4. Comparison of observed and modelled nitrate, ammonium, sulfate and organic
946 aerosol at Payerne for March 2009.

947

948

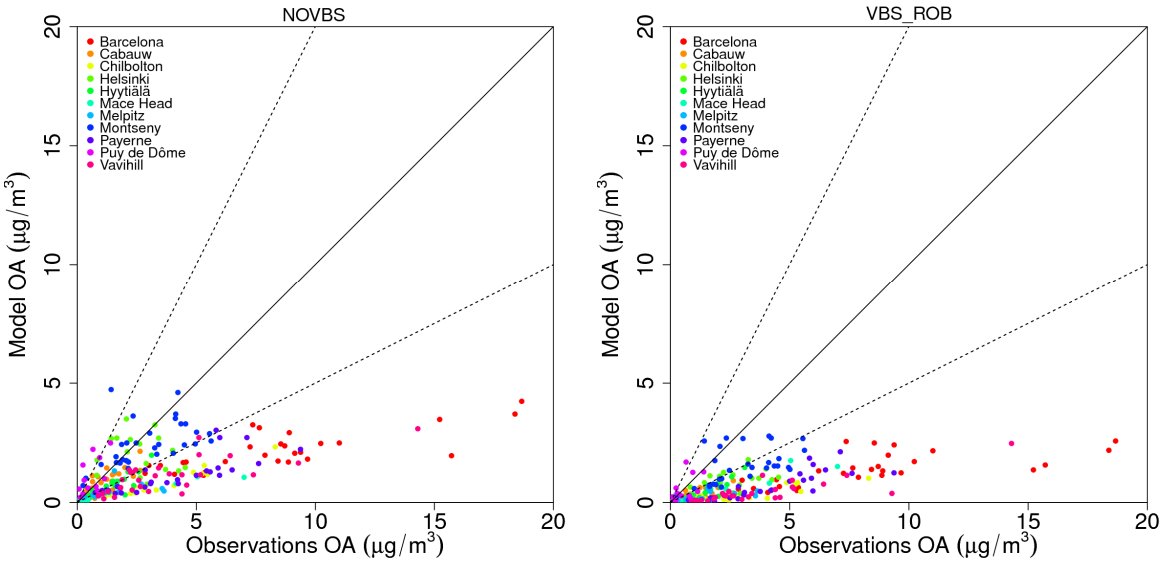

949

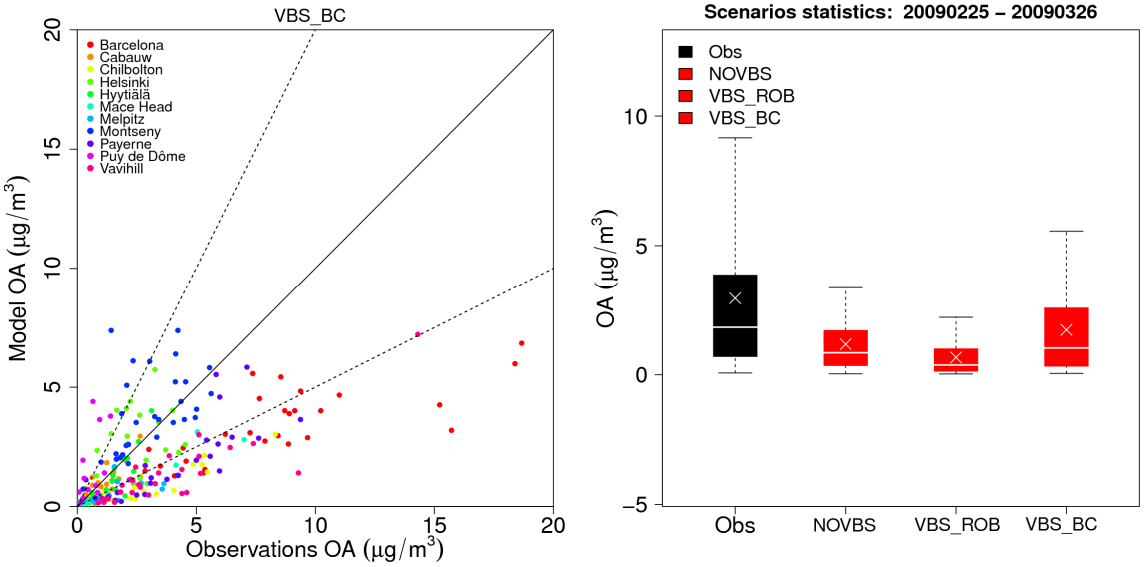

950 Figure 5. OA daily average scatter plots for NOVBS, VBS_ROB and VBS_BC scenarios for
951 February-March 2009 for stations in Table 3. Solid lines indicate the 1:1 line. Dotted lines are
952 the 1:2 and 2:1 lines. Boxplots indicate medians, 5th, 25th, 75th and 95th quantiles for
953 observations (black) and sensitivity tests (red). The crosses represent the arithmetic means. R^2
954 is 0.55 for NOVBS, 0.64 for VBS_ROB and 0.59 for VBS_BC (excluding the elevated sited
955 of Puy de Dôme and Montseny).

956

957

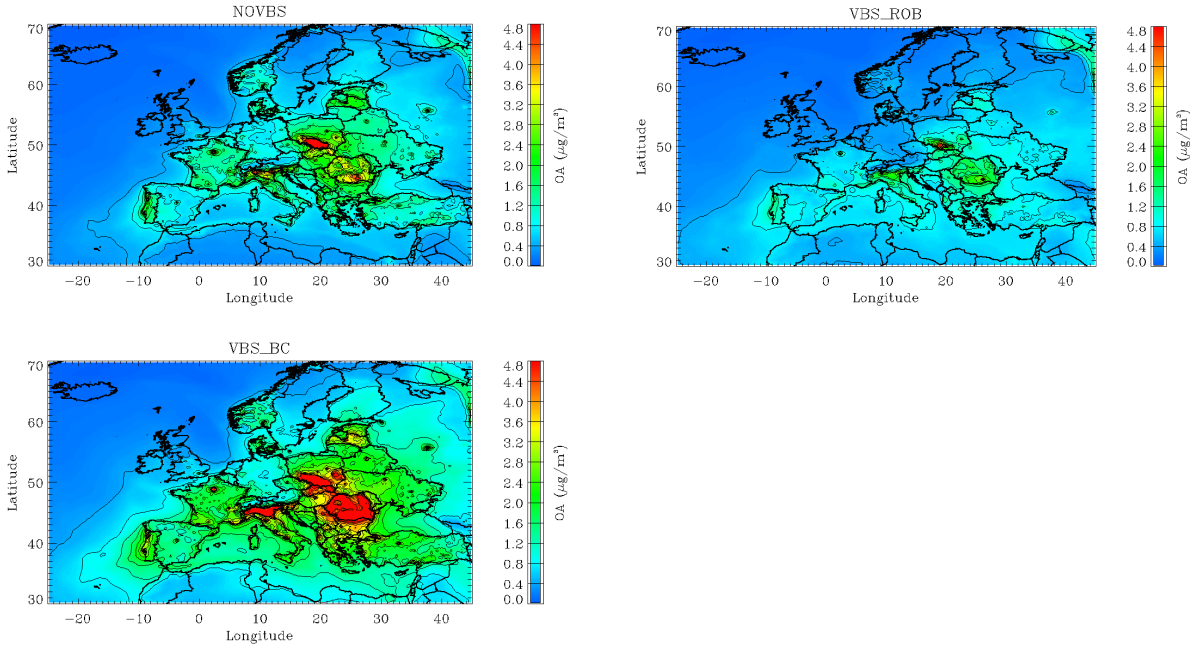

958

959 Figure 6. Predicted OA concentrations over Europe for the NOVBS, VBS_ROB and
960 VBS_BC scenario in February-March 2009. Note that the color scale was limited to
961 maximum of 4.8 μg/m^3 to facilitate comparison of the panels.

962

963

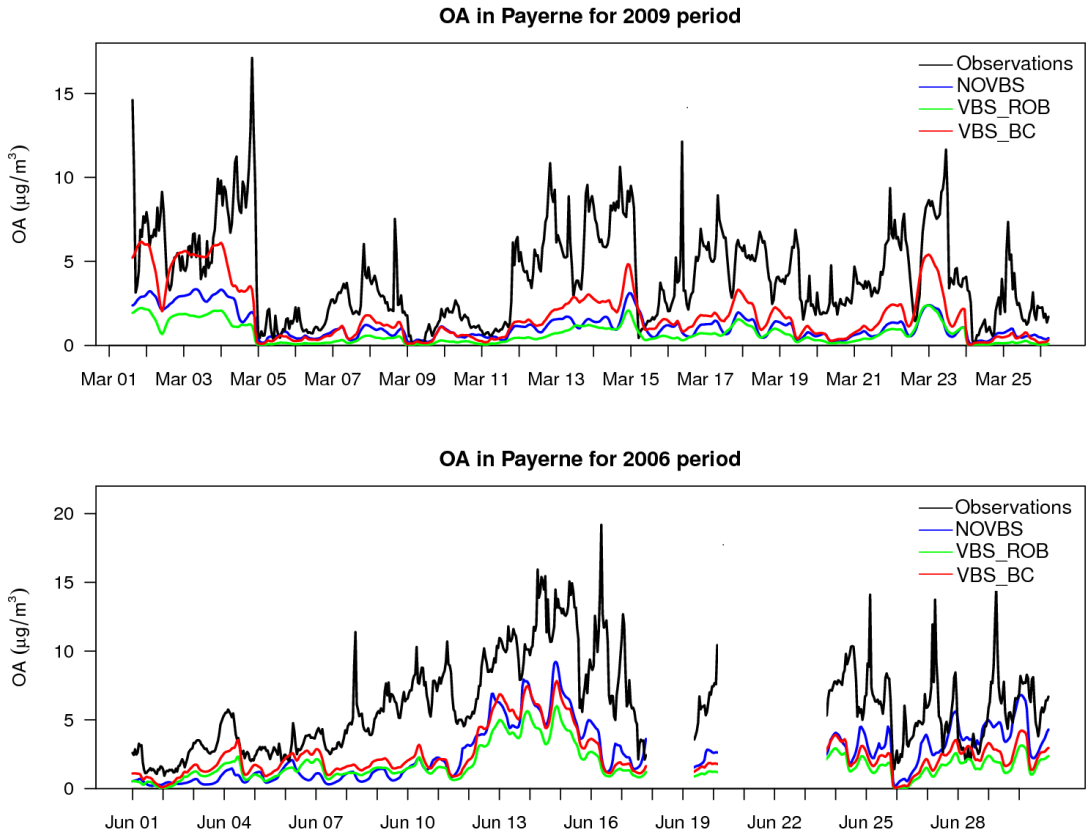

964

965 Figure 7. Predicted and observed total OA for scenarios NOVBS, VBS_ROB and VBS_BC in
966 March 2009 (upper panel) and June 2006 (lower panel) at Payerne.

967

968

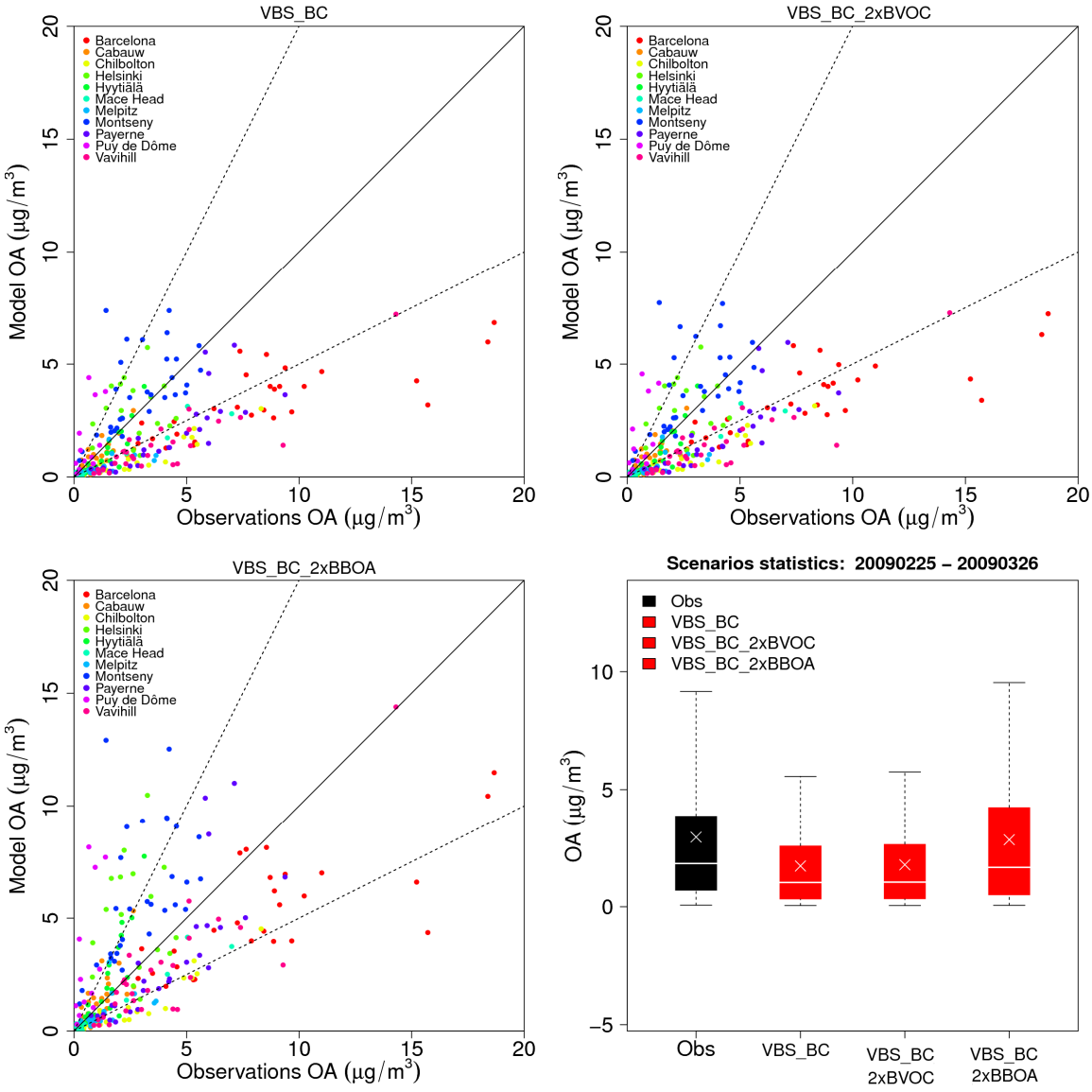

969

970 Figure 8. OA daily average scatter plots for VBS_BC, VBS_BC_2xBVOC and
971 VBS_BC_2xBBOA scenarios for February-March 2009 for stations in Table 3. Solid lines
972 indicate the 1:1 line. Dotted lines are the 1:2 and 2:1 lines. Boxplots indicate medians, 5th,
973 25th, 75th and 95th quantiles for observations (black) and sensitivity tests (red). The crosses
974 represent the arithmetic means.

975

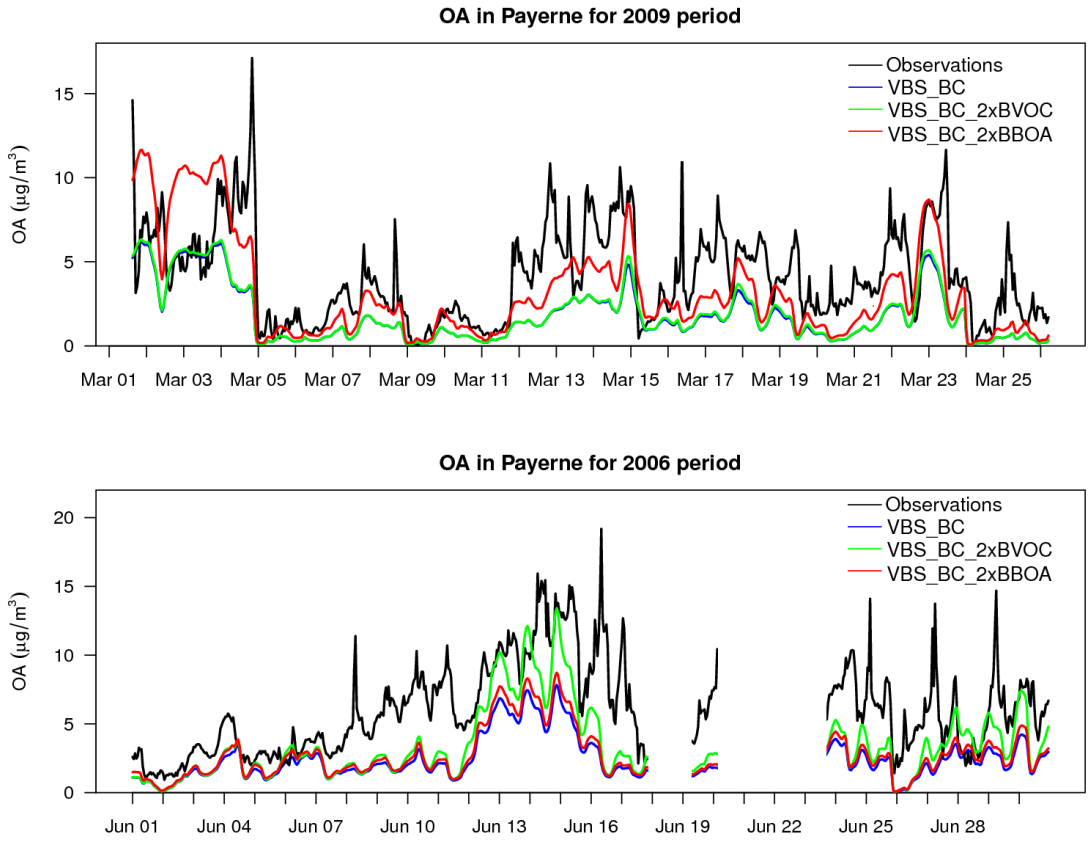

Figure 9. Predicted and observed total OA for scenarios VBS_BC, VBS_BC_2xBVOC and VBS_BC_2xBBOA in March 2009 (upper panel) and June 2006 (lower panel) at Payerne.

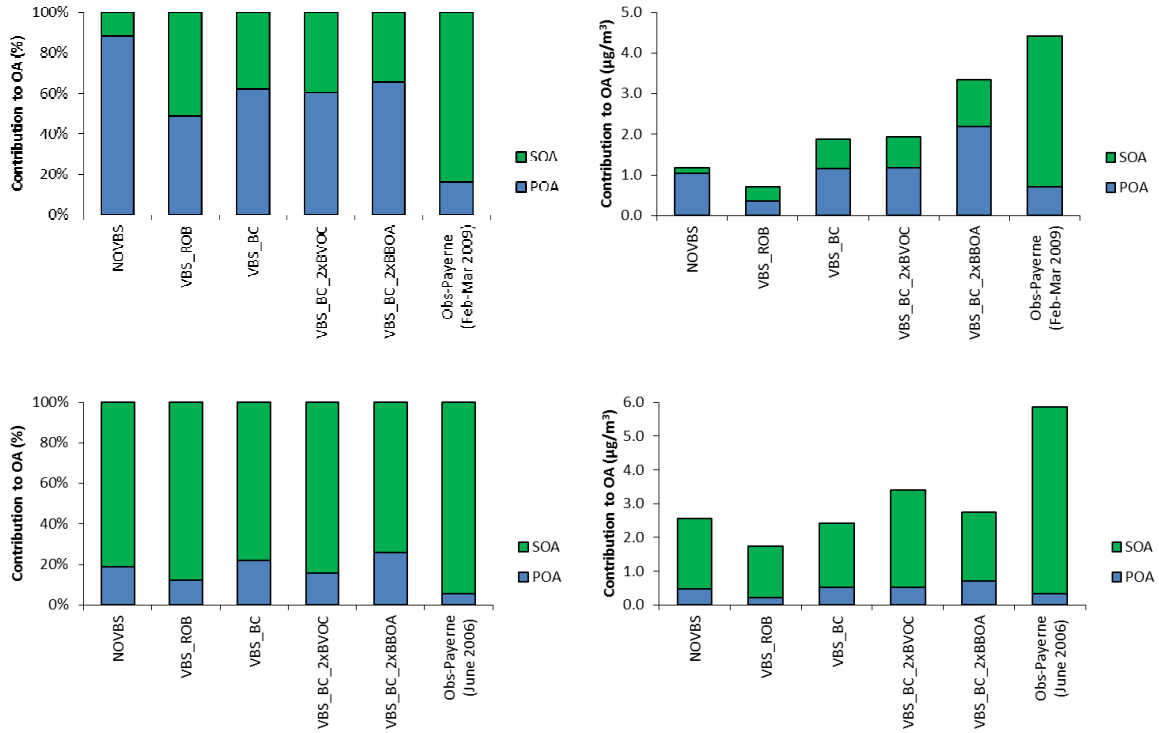

Figure 10. Relative (left) and absolute (right) contribution of predicted and measured POA and SOA fractions to the total OA mass at Payerne for February-March 2009 winter period (upper-panel) and June 2006 (lower-panel) and different model scenarios. NOVBS: (traditional non-volatile POA), VBS_ROB (Robinson et al., 2007), VBS_BC (Tsimpidi et al., 2010, Shrivastava et al., 2011), VBS_BC_2xBVOC (increased biogenic emissions relative to VBS_BC), VBS_BC_2xBBOA (increased biomass burning emissions relative to VBS_BC), Obs-Payerne: AMS-PMF.